Renewable and Sustainable Energy Reviews 199 (2024) 114502

Contents lists available at ScienceDirect

Renewable and Sustainable Energy Reviews

journal homepage: www.elsevier.com/locate/rser

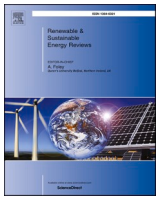

A comprehensive review on the similarity and disparity of torrefied biomass and coal properties

Adekunle A. Adeleke [a,**], Peter P. Ikubanni [b,*], Stephen S. Emmanuel [c], Moses O. Fajobi [d], Praise Nwachukwu [b], Ademidun A. Adesibikan [c], Jamiu K. Odusote [e], Emmanuel O. Adeyemi [f], Oluwaseyi M. Abioye [g], Jude A. Okolie [h]

[a] Department of Mechanical Engineering, Nile University of Nigeria, Abuja, Nigeria
[b] Department of Mechanical Engineering, Landmark University, Omu-Aran, Nigeria
[c] Department of Industrial Chemistry, University of Ilorin, Ilorin, Nigeria
[d] Department of Mechanical Engineering, Ladoke Akintola University of Technology, Ogbomoso, Nigeria
[e] Department of Materials and Metallurgical Engineering, University of Ilorin, Ilorin, Nigeria
[f] Department of Mechanical Engineering, Bells University, Ota, Nigeria
[g] Department of Agricultural and Biosystems Engineering, Landmark University Omu Aran, Nigeria
[h] Gallogly College of Engineering, University of Oklahoma, USA

ARTICLE INFO

Keywords:
Torrefaction
Torrefied biomass
Coal
Renewable energy
Hydrophobic
Grindability

ABSTRACT

The use of coal for energy generation is facing serious scrutiny because of environmental concerns. As a result, there is a growing global interest in biomass, a renewable and readily available energy source. However, the utilization of biomass comes with significant drawbacks, including its heterogeneity, low bulk density, and calorific value. Biomass also has a low energy content, high moisture, poor grindability, and high volatile matter, which affect its handling, bulk transportation, and storage. Torrefaction technology has been employed in previous works to improve the properties of biomass for subsequent handling and transportation and for low-cost energy generation. Since coal is a promising precursor for energy generation, it is imperative to compare the physicochemical properties of coal with that of torrefied biomass. Therefore, this study aims to conduct a comprehensive comparison between various grades of coal and torrefied biomass. The review revealed that torrefied biomass could replace coal, as its properties are similar to those of coal, except for high-grade coals. The proximate and ultimate analyses of coals (lignite and bituminous) were found to be comparable to various torrefied biomass materials. The fuel ratio (0.5–2.0), and higher heating values (16,100–19,000 kJ/kg) of coal and torrefied biomass were within the range useful for coal-fired plants. Additionally, ash analyses, ash fusion temperature, hygroscopic tendency, functional group study, and microstructural comparison were reviewed in this study. The results from various studies have shown close similarities with only small disimilarities in the fuel properties between coal and torrefied biomass. Therefore, torrefied biomass is proposed as a complimentary feedstock to coal in various applications.

1. Introduction

Torrefaction is a thermochemical conversion process that subjects biomass to thermal treatment to produce high-quality solid biofuel [1]. The resulting fuels are reported to exhibit combustion properties comparable to those of fossil fuels, especially coal. Coal, a prominent primary fossil fuel, is characterized by its carbon content and typically exhibits a brownish appearance [2]. The use of coal in various applications is accompanied by several hazards, beyond those related to its mining and preparation. A significant challenge is the pollution resulting from the use of coal, as the emitted gases are toxic and harmful, posing a threat to the stability of the ecosystem [3].

Due to the carbon richness of coal, which has been widely acknowledged, concerted efforts have been geared towards finding better alternatives, especially the ones that will be suitable and serve the same purpose as coal does. In addition, the fact that coal is a non-renewable source of energy poses a serious concern to its continuous

* Corresponding author.
** Corresponding author.
E-mail addresses: adekunle.adeleke@nileuniversity.edu.ng (A.A. Adeleke), ikubanni.peter@lmu.edu.ng (P.P. Ikubanni).

https://doi.org/10.1016/j.rser.2024.114502
Received 14 March 2023; Received in revised form 13 April 2024; Accepted 29 April 2024
Available online 9 May 2024

Abbreviations **meaning**

A	Ash
C	Carbon
DT	Deformation Temperature
EMC	Equilibrium Moisture Content
FC	Fixed Carbon
FR	Fuel Ratio
FT	Final Fusion Temperature
FTIR	Fourier Transform Infrared
H	Hydrogen
H/C	Hydrogen/Carbon
HGI	Hardgrove Grindability Index
HHV	High Heating Value
HT	Hemispherical Temperature
HTM	Highly Torrefied Material
IDT	Initial Deformation Temperature
LTM	Lightly Torrefied Material
M	Moisture
N	Nitrogen
NR	Not Recorded
O/C	Oxygen/Carbon
O_2	Oxygen
RB	Raw Biomass
S	Sulfur
SEM	Scanning Electron Microscopy
ST	Softening Temperature
TB	Torrefied Biomass
TTBGI	Thermally Treated Biomass Grindability Index
VM	Volatile Matter
WDPT	Water Drop Penetration Time
Symbols and Units	Meaning
%	Percentage
kJ/kg	Kilojoule per kilogram
^{o}C	Degree Celcius
wt.%	Weight percent
cm^{-1}	Per unit centimetre
h	Hour
min	Minute
MW	Megawatt
kW	Kilowatt
Θ	Static Water Contact Angle
Subscript	Meaning
el	Electric
th	Thermal

utilization. Moreover, the consistent use of coal in power plants worldwide has brought it close to extinction just like any other non-renewable energy, thus justifying the need for other eco-friendly alternatives [3].

Biomass, especially lignocellulosic materials, stands out as a promising substitute for coal due to its renewable nature and the ability to provide a similar energy output while significantly reducing greenhouse gas emissions [4,5]. Annually, approximately 181.5 billion tonnes of lignocellulosic biomass, including crop residues, wood, and grass, are produced globally justifying its availability [1]. Considering the constantly increasing world population (annual growth rate of 1.09 %) and energy consumption (2 % each year), biomass energy utilization could contribute towards addressing the energy demand of the world [6,7]. However, lignocellulosic biomass is characterized by its heterogeneous composition, hygroscopic nature, low calorific value, and low bulk density [5,6]. These characteristics pose challenges during handling, bulk transportation, and storage. To mitigate these issues, torrefaction processes are employed as pretreatment methods to enhance the properties of biomass materials for easier handling, transportation, and conversion into fuels and value-added chemicals. It is important to note that torrefaction does not replace conventional methods like gasification and pyrolysis; rather, it serves as a complementary method to improve biomass properties for its subsequent use in producing green fuels and sustainable chemicals.

Several researchers have performed torrefaction studies on various biomass for solid fuels production [3,8–10]. For instance, Nunes et al. [3] presented a case study that demonstrates the practical application of torrefied biomass in power plants. Adeleke et al. [9] reported a comprehensive review of torrefaction as a promising biomass pretreatment strategy. The authors noted the potential areas where torrefied biomass could be useful including densification into pellets and briquettes as well as energy generation [9]. Chen et al. [10] compared the gasification performance of raw biomass, torrefied biomass, and coal. Their results reveal that torrefaction significantly enhances the gasification performance of biomass for syngas production. Additionally, excellent reviews related to biomass torrefaction have been reported in literature [11–13]. For instance, Chen et al. [11] reported recent advances and progress in biomass torrefaction. The authors performed a detailed review of literature and discussed the trends in practical torrefaction development and environmental performance [11]. In another detailed review, Thengane et al. [12] focus on the kinetics, particle and reactor scale models, and reactor designs of biomass torrefaction systems. Tumuluru et al. [13] presented a comprehensive review of studies that reported the influence of torrefaction on product quality in terms of the physicochemical composition and storage behavior of the biomass. Despite the significant body of literature on biomass torrefaction, a comparative analysis of the combustion and fuel properties as well as the physicochemical properties of torrefied biomass and various types of coal is scarcely reported in literature. While the majority of the previous studies concluded that torrefied biomass is a clean energy source, which is the aim of the United Nations' Sustainable Development Goal 7 (SDG 7). They do not present information on how biomass torrefaction improves the properties of biomass comparable to that of coal. It should be noted that the suitability of any fuel for power generation requires an in-depth understanding of its combustion and fuel properties. This knowledge guides users in applying the fuel for specific purposes effectively. Therefore, the present study attempts to fill the knowledge gaps by providing a meticulous review of the literature to compare the combustion, fuel, and physicochemical properties of coal and torrefied biomass. These comparisons are crucial to understand their efficiency, environmental impact, and suitability for energy production in a transition towards more sustainable fuel sources. The aim of the study is achieved by reviewing a wide range of studies and by comparing previous findings on torrefied biomass and various types of coal. This comparison will assist in guiding pilot and industrial experiments, proving highly beneficial to industries and policymakers who are considering the adoption of torrefied biomass as a partial or complete substitute for coal in energy and metallurgical applications. Based on these considerations, the suitability of torrefied biomass as an effective replacement for coal has been established. The entire study is structured as follows: Section one describes the introduction while sections 2–4 provide a comparative analysis of the fuel and combustion properties as well as the physicochemical properties of biomass and coal. Section 5 introduces the FTIR comparison as a means of juxtaposing between the functional groups. Section 6 compares the hydrophobicity property. Sections 7 and 8 compare the physical properties such as grindability and visible microstructure. Section 9 compares various energy applications of coal and torrefied biomass. The final section provides the

authors perspectives, conclusions, and recommendations for future studies.

2. Comparative analysis of the proximate, ultimate, heating values, and compositional analysis of coal and torrefied biomass

The properties of biomass and coal with respect to location, species type, cultivation, processing conditions, torrefaction approach, and or refining strategy are non-homogeneous. In this regard, the energy research community has pragmatically established that extracting information from fuel to parametrically have a better understanding of its behavior as per elemental composition, elemental stoichiometry, thermal properties, combustibility, and flammability is important. These will serve as pointers to the performance and environmental risks involved in their usage. For instance, the N and S contents are significant pointers to NO_x and SO_x emissions [1].

The evaluation of combustion, co-combustion, devolatilization, and decomposition behaviour can be conducted through three fundamental measurements: proximate and ultimate analysis as well as the heating value analysis. In exploring the potential of producing charcoal from coconut shells, proximate, ultimate, and heating value analyses were performed by Kabir et al. [2]. These analyses, also conducted on torrefied biomass for coal-fuel power plants [3], coal and non-woody biomass [4], forest tree species [5], *Megathyrsus maximus* [6], selected lignocellulosic biomass [7], and *Digitaria sanguinalis* [8], demonstrated that biomass can be a useful source of clean energy, helping to prevent the release of toxic emissions [9].

Proximate analysis is a key method for evaluating and characterizing biomass and coal for thermal conversion. It reveals the percentage proportion of the material that combusts in the solid state (fixed carbon), in a gaseous state (volatile matter), and the percentage of the inorganic waste material (ash content) alongside the percentage of moisture [10]. Several studies have reported the proximate, ultimate, and HHV analyses of various biomass materials [14–16]. These include Malaysian oil palm waste [14], municipal solid waste [15], distillery sludge and bio-compost [16], lignocellulose biomass [17], sewage sludge and beverage waste [18], orange bagasse [19], banana pseudo-stem [20], and coppice willow [21]. Evaluating these properties is crucial because they significantly affect combustion processes and the design of plant infrastructure, making them highly relevant for fuel usage [22].

Compared to the proximate analysis, the higher heating value (HHV) assessment shows the amount of energy in biomass or coal that is released as thermal energy upon combustion, and this determines the energy value of a fuel [23]. The HHV governs the fuel's energy potential and potential as feedstock for subsequent thermochemical conversion processes [24]. Hence, it serves as a key parametric factor in the evaluation and choice of biomass material as a source of fuel [25,26]. Studies have shown that the predictions of HHV of biomass are actualizable through different techniques including regression analysis [24], machine learning algorithms [27], support vector machines [28], and experimental methods [29]. The HHV obtained in a study by Bot et al. [30] and Inayat et al. [31] revealed the potential energy achievable when the biomass is used as briquettes. The HHV of municipal solid waste was also modeled by Ibikunle et al. [32]. It should be noted that pyrolysis process parameters have an influence on the HHV of biomass [33]. Thus, HHV plays a crucial role in the operational process layout [34], mathematical modeling [35,36], predictions [37,38], and simulation analysis of energy plants [39].

Ultimate analysis is another important biomass characteristics that reveal information about the elemental composition of biomass [40] as well as its quality [41,42]. It is employed to quantify the percentage of hydrogen, nitrogen, oxygen, carbon, sulfur, and sometimes chlorine and fluorine in biomass and coal [43,44]. The ultimate analysis is useful in predicting the HHV of biomass [45]. This ultimate analysis is also essential for gasification processes because it enables the determination of the volume of steam needed and the H/C ratio of a fuel [46,47]. Ultimate analysis is also essential for assessing its energy content and environmental impact upon combustion.

The proximate and ultimate analyses performed on biomass, torrefied biomass, and coal provide baseline information for evaluating their effectiveness and applicability for power generation [48,49]. While compositional analyses of biomass such as hemicellulose, cellulose, and lignin determination are essential in evaluating its suitability for biofuel production, evaluating the proximate, ultimate, and HHV are also useful to predict biomass energy utilization potential [50]. Biomass can be used for energy generation or biofuel production through processes such as hydrothermal liquefaction [51], thermal process [52], thermochemical processes [53], and plasma co-gasification [54]. Both biomass (raw and torrefied) and coal could be used as precursors for these processes. Therefore, they are characterized for their physiochemical properties [55], and combustion properties [56], while non-isothermal kinetic parametric evaluations are also performed [57,58] prior to their utilization.

In a study by Singh et al. [59], pet coke was mixed with rice straw to produce fuel for power generation. The physicochemical and combustion characteristics of the fuel developed were investigated. The findings reveal that while pet coke is a great precursor for power generation, its combination with rice straw is more desirable. Empirically speaking from the survey of diverse studies, torrefied biomass (TB) and coal share some similarities as the torrefaction process improves the quality of biomass. The disparities between TB and coal as fuel have been almost infinitesimal as rigorous efforts are deployed to ensure that TB outmatches coal fuel quality to boost the actualization of sustainable development goals number seven (7) and eleven (11). The goals aimed at ensuring access to clean and affordable energy in cities that are inclusive, safe, resilient, and sustainable. For example, in a co-firing comparative study conducted by Sher et al. [60], it was reported that there is appreciable dissimilarity in the percentages of FC, ash, and VM of the two torrefied (low and medium temperature) beech wood compared to EI Cerrejon coal.

It has been noted that an increase in ash content can raise the operating and maintenance costs of combustors while decreasing the HHV. The ash content of low-temperature biomass was reported to be 1.12 %, slightly lower than that of high-temperature beech wood (1.15 %). This is significantly lower than the ash content in El Cerrejon coal, which stands at 14 %, indicating the suitability of TB for combustion. Moreover, TB has a low sulfur content (<0.03 %) compared to approximately 0.5 % in El Cerrejon coal, as revealed in the ultimate analysis. A notable disparity in elemental composition and proximate analysis was also observed by Trubetskaya et al. [61] between anthracite coal, torrefied olive stems, and woodchips. According to their analyses (presented in Tables 1 and 2), anthracite coal is less volatile and less reactive than torrefied olive stems, due to its higher carbon percentage. However, the nitrogen level in anthracite coal (1 %) is comparable to that of the torrefied olive stem (1 %), whereas its sulfur content is higher, similar to El Cerrejon coal, compared to the torrefied olive stem and woodchip [61].

Panahi et al. [67] also explored six TB (Corn straw, Miscanthus, Sugar-cane bagasse, Distiller's Dried Grains with Soluble-DDGS, Rice husk, and Beechwood) for co-firing. The result of HHV and proximate analyses are in line with those reported for torrefied Annona squamosa peel [63], Sugarcane bagasse [94], barley straw and cumin stalks [98], and passion fruit peel waste and pineapple peel waste [74]. However, these results differ from the reported data of Inner Mongolia lignite, Jinjie bitumite, and Ningxia anthracite coal [88] and are in very close range with that of Utah bituminous coal [82], Kaltim prima and Sinjai Indonesia coal [81].

In the ultimate analysis of the six types of torrefied biomass (TB), only Miscanthus and DDGS exhibit high sulfur contents of 0.47 % and 1.00 %, respectively, levels that are roughly equivalent to those of most coals as reported in Table 2. The parametric values for beech wood fuel

Table 1
Comparative proximate analysis, fuel ratio, and higher heating value of different torrefied biomass and coal samples. Note that[a] indicates wet basis while all others represents dry basis.

Fuel sample	A (%)	FC (%)	M (%)	VM (%)	FR	HHV (kJ/kg)	References
Torrefied biomass							
Mangifera indica seed[a]	16.70	4.70	NR	78.60	0.06	29,000	[62]
Annona squamosa peel	7.60	10.50	NR	82.00	0.13	23,300	[63]
Passiflora edulis shell[a]	10.10	11.50	NR	78.30	0.15	26,000	[62]
Passiflora edulis shell	11.23	13.0	NR	78.30	0.15	26,000	[62]
Pine wood chips	1.02	15.70	5.70	77.60	0.20	NR	[64]
Rubber wood	3.60	17.90	NR	78.60	0.23	21,390	[65]
Bamboo wood chips	1.45	20.70	6.40	71.50	0.29	NR	[64]
Mango seeds	7.80	20.74	NR	71.45	0.29	24,842	[66]
Avocado seeds	9.90	20.74	NR	69.36	0.30	26,513	[66]
Oak wood chips	0.47	21.00	3.20	75.40	0.28	NR	[64]
Low-temperature torrefied beech wood	1.12	21.00	3.00	77.88	0.27	21,058	[60]
Corn DDGS	7.45	21.09	NR	71.46	0.30	23,700	[67]
Rice husk	22.80	21.58	NR	55.62	0.39	16,100	[67]
Groundnut stalk[a]	5.54	21.59	2.01	70.86	0.31	19,680	[68]
Groundnut stalk	5.86	27.53	2.05	70.86	0.31	19,680	[68]
Spent coffee grounds	1.35	21.89	NR	76.76	0.29	22,420	[69]
Miscanthus	2.70	22.30	NR	75.00	0.30	20,100	[67]
Sugarcane bagasse	2.71	23.49	NR	73.74	0.32	20,300	[67]
Ananas comosus peel	9.70	23.90	NR	66.40	0.36	27,700	[63]
Wheat straw[a]	14.90	23.90	2.50	58.57	0.41	18,760	[68]
Wheat straw	17.50	31.40	2.56	58.57	0.41	18,760	[68]
Corn straw	7.89	24.56	NR	67.55	0.36	19,400	[67]
Gliricidia wood	9.20	25.50	NR	65.3	0.39	22,440	[65]
Medium temperature torrefied beech wood	1.15	27.00	2.38	71.85	0.38	21,698	[60]
Beechwood	0.50	27.30	NR	72.20	0.39	20,900	[67]
Spent coffee grounds	0.86	28.30	NR	70.80	0.40	29,500	[70]
lychee seeds	10.81	32.47	NR	56.71	0.57	25,241	[66]
Palm kernel shell[a]	5.22	35.00	8.40	51.40	0.68	22,280	[71]
Rice husk	23.40	35.30	NR	41.30	0.85	19,000	[50]
Olive kernel	3.90	37.8	4.0	54.3	0.70	25,497	[72]
Canola residue	10.40	39.90	0.2	49.60	0.80	22,300	[73]
Passion fruit peel waste	14.02	40.19	3.88	45.79	0.88	20,780	[74]
Sugar cane bagasse	3.95	44.04	NR	51.85	0.85	24,010	[75]
Sugarcane leaves	20.09	46.53	2.36	31.03	1.50	21,610	[76]
Rubberwood	3.83	52.42	0.73	43.75	1.20	27,170	[77]
Pineapple peel waste	8.10	52.95	3.73	38.95	1.36	22,970	[74]
Sugarcane bagasse	6.32	57.29	1.21	35.18	1.63	25,240	[76]
Acacia nilotica wood	1.87	60.40	0.88	36.84	1.64	24,760	[78]
Patula pine	0.93	70.48	NR	28.59	2.47	23,900	[79]
Coconut Shells	0.81	83.90	1.10	14.20	NR	32,150	[80]
Coal							
Sinjai coal	52.41	13.96	10.09	23.54	0.59	16,489	[81]
Kaltim Prima Coal	3.77	37.01	16.11	43.10	0.86	17,409	[81]
Utah bit	16.20	37.60	4.15	42.00	0.89	24,500	[82]
Wucaiwan coal	4.89	46.98	14.88	33.25	1.41	NR	[83]
Tianchinengyuan coal	4.10	47.77	18.54	29.59	1.61	NR	[83]
Sebuku bit.	12.10	47.90	0.90	39.10	1.23	27,650	[71]
Bit	13.44	49.72	0.92	35.92	1.38	29,868	[84]
Wudong coal	15.46	51.13	2.97	30.44	1.68	NR	[83]
Shenmu bit	7.68	52.31	8.12	31.89	1.64	24,440	[85]
Shenmu-shaanxi bit	11.18	52.52	7.98	28.32	1.85	21,480	[86]
Tangkou bit	9.83	53.00	2.32	34.85	1.52	NR	[87]
Jinjie bit	9.67	54.67	3.58	36.98	1.48	30,820	[88]
EI Cerrejon bit	14.00	55.00	2.25	31.00	1.77	28,134	[60]
Colombian hv bit	0.70	56.10	NR	43.20	1.30	32,200	[89]
Inner Mongolia lig	10.96	56.58	3.86	33.58	1.68	30,230	[88]
Hefeng sub	21.18	57.19	5.88	42.81	1.34	NR	[90]
Shengli lig	9.48	61.81	17.50	38.19	1.62	NR	[91]
Changping lv bit	27.58	62.87	1.86	8.49	NR	24,940	[92]
Shaanxi lv bit	4.89	65.64	4.61	34.36	1.91	NR	[93]
Jincheng ant	16.11	77.83	2.78	3.28	NR	26,110	[85]
Ningxia ant	6.70	84.99	0.82	8.10	NR	33,110	[88]

NR = not recorded, ant-anthracite, lv, low volatile, bit-bituminous.
[a] = wet basis; A = ash; FC = fixed carbon; M = moisture; VM = volatile matter; FR = fuel ratio; Note that the wet basis has been converted to dry basis using the expression: $M_{dry} = M_{wet}\ (100/(100\text{-}M_{dry}))$. Where M_{dry} and M_{wet} represent the property of the dry and wet basis respectively.

align with those reported by Sher et al. [60]. Additionally, unlike the other coals and TB listed in Table 1, Kaltim Prima and Sinjai coals [88] have a notably high moisture content. Sinjai coal [88] and torrefied rice husk [67] are characterized by a high ash content, which could complicate their management in terms of shipping, stowing, grinding, combustion, and the potential for environmental pollution [81].

Among the fuel samples listed in Table 1, Zhundong coal properties reported by Xin et al. [101] stands out with an unmatched HHV of 54, 630 kJ/kg. However, its moisture content remains a concern, similar to that of Shengli lignite [91], and Kaltim Prima and Sinjai coal [88]. Xiao

Table 2
Comparative ultimate analysis of different torrefied and coal samples. Note that * indicates wet basis while all others represent dry basis.

Fuel sample	C (%)	H (%)	N (%)	O (%)	S (%)	References
Torrefied biomass						
Groundnut stalk*	41.20	8.70	1.19	47.70	1.15	[68]
Oak wood chips	49.99	5.88	2.68	41.25	NR	[64]
Sugarcane bagasse	50.30	3.40	0.22	45.79	0.29	[94]
Bamboo wood chips	52.11	5.68	3.35	38.86	NR	[64]
Hibiscus cannabinus L	52.27	5.27	0.87	41.49	0.11	[95]
Rubber wood	53.50	6.70	NR	39.80	NR	[65]
Pepper stem*	55.00	6.80	2.30	35.8	NR	[96]
Pine wood chips	55.28	5.79	2.77	36.16	NR	[64]
Beechwood	55.40	5.30	0.18	38.88	0.31	[67]
Willow	55.50	3.64	1.30	42.20	NR	[97]
Wheat straw	55.50	3.64	1.30	44.70	NR	[97]
Woodchip	55.50	5.00	0.03	38.50	0.02	[61]
Passion fruit peel waste	56.71	4.41	1.11	37.77	0.00	[74]
Cumin stalks	58.00	3.87	1.04	36.97	0.12	[98]
Sugar cane bagasse	58.25	2.81	0.31	38.68	0.15	[75]
Rapeseed straw	58.50	4.24	1.74	45.5	NR	[97]
Wood waste	59.66	4.73	0.45	35.14	0.02	[98]
Gliricidia wood	59.70	5.70	NR	34.60	NR	[65]
Coffee chaff	60.20	5.70	4.00	30.00	NR	[99]
Barley straw	61.18	3.81	1.37	33.51	0.13	[98]
Pineapple peel waste	61.37	4.37	1.30	32.96	0.00	[74]
Annona squamosa peel	61.90	4.60	2.60	30.50	0.40	[63]
Ananas comosus peel	64.10	4.50	1.10	30.00	0.30	[63]
Acacia nilotica wood	64.75	4.85	0.64	29.76	NR	[78]
Rice straw	65.16	5.61	1.41	27.83	NR	[100]
Spent coffee grounds	66.60	7.50	2.70	23.10	0.1	[70]
Spent coffee grounds	69.60	7.10	3.60	19.6	NR	[99]
Patula pine	76.03	3.75	0.35	19.87	NR	[79]
Coal						
Zhundong sub	65.50	4.60	0.16	29.33	0.42	[101]
Shengli lig	70.07	4.45	0.97	23.06	1.45	[91]
Okaba sub	71.47	2.88	0.90	24.04	0.71	[102]
Okaba sub	71.47	2.88	0.90	24.04	0.71	[103]
Okaba sub	71.47	2.88	0.90	24.04	0.71	[104]
Hefeng sub	72.55	5.73	1.46	19.38	0.88	[90]
Tangkou bit	73.34	5.60	1.54	19.09	0.43	[87]
Jhama coal	73.43	2.51	1.31	22.04	0.71	[105]
EI Cerrejon bit	78.50	5.98	1.57	13.48	0.47	[60]
Shaanxi lv bit	81.89	4.73	1.08	12.01	0.29	[93]
Changping lv bit	89.38	3.18	1.36	5.65	0.43	[92]
Vietnamese ant	90.57	3.06	1.37	4.15	0.85	[95]

Note that the wet basis has been converted to dry basis using the expression: $M_{dry} = M_{wet}$ (100/(100-M_{dry})). Where M_{dry} and M_{wet} represent the property of the dry and wet basis respectively.

et al. [83] also investigated three types of coal (Wucaiwan, Tianchinengyuan, and Wudong coals). The coals were very similar in empirical and elemental properties, except that the Wucaiwan and Tianchinengyuan coal have high moisture contents while Wudong coal has high ash content [83]. However, there are huge dissimilarities in both properties of the three coals when compared to torrefied spent coffee grounds [69], especially with the FC, VM and oxygen contents reported as 21.89 %, 76.76 % and 36.88 % respectively (see Tables 1 and 2). Interestingly, the properties of torrefied spent coffee grounds recorded by Nepal et al. [69] are consistent with those reported by Barbanera and Muguerza [70] and Sermyagina et al. [106], but lower in HHV when compared with spent coffee grounds (29,500 kJ/kg) [70], and marula seeds (27, 900 kJ/kg) [107]. It is also lower compared with that of Melina wood (31,080 kJ/kg) and teak wood (28,860 kJ/kg) [108]. The torrefied biomass has closely related HHV with some of the coals reported in Table 1.

Chen and Jhou [109] investigated the production of biofuels that were analogously comparable to coal to lessen reliance on fossil fuels. The biofuels' comparativeness to coal was assessed by juxtaposing their HHV, element composition, proximate analysis data, and combustibility profile. The study empirically established that there was a striking parallelism of about 55 % and that the most comparable sample was the one containing an equal mixture of torrefied pine sawdust and spent coffee grounds, which was 62 % the same as coal. Similarly, Chen et al. [110] established in their study that the closeness of the disparity gap between TB and coal is a function of the torrefaction temperature.

The chemical composition including the cellulose, hemicellulose and lignin of TB and coal is also compared and presented in Fig. 1 [110]. The figure displays the chemical composition of both raw and torrefied rice husks. The rice husk torrefied at 300 °C showed an elemental composition similar to that of lignite and peat coal, unlike rice husk samples torrefied at lower temperatures (210, 240, and 270 °C). This similarity is attributed to the decomposition of cellulose, which enhances the carbonization outcome of the rice husk and increases the percentage of FC in the torrefied rice husk [111]. This observation aligns with findings on torrefied gliricidia and rubber wood, as illustrated in Fig. 2 [65], and torrefied wood [112].

Fig. 2 displays the HHV of raw and torrefied gliricidia and rubber wood at different times and temperatures. Poudel et al. [112] observed that at 300 °C, the torrefied waste wood came in the range of lignite with improved HHV and CHO values, and reduced ash composition. However, the observation of Singh et al. [78] differs because the ash content increases as the FC content increases after *Acacia nilotica* wood was torrefied. The partial difference was further solidified by the fact that devolatilization of *Acacia nilotica* wood skyrockets with an upsurge in temperature which leads to a proportionate diminution in percentage moisture and volatile matter contents and a comparative upsurge of FC and ash quantity of *Acacia nilotica* wood [78]. More specifically, during torrefaction, there is a fall in the O/C proportion of biomass. This is attributed to increased lignin ($C_9H_{10}O_2$, $C_{10}H_{12}O_3$, $C_{11}H_{14}O_4$) composition which has a low O/C proportion in contrast to the proportion of O/C that is in hemicellulose $(C_5H_8O_4)_n$ and cellulose $(C_6H_{10}O_5)_n$ [50]. This low O/C ratio can be attributed to the reduction in O_2 that invariably results in elemental carbon dominance. Consequently, this leads to an upsurge in the HHV profile of the TB [74]. This explanation is corroborated by using the carbon enrichment data presented in Fig. 3. Silva et al. [74] reported zero sulfur for torrefied passion-fruit-peel and pineapple peel wastes. The torrefaction temperature had a significant influence on the energy profile of the torrefied solids from agro-industrial leftovers, which had properties analogous to lignite and peat [74].

The opinion of this review is that 100 % of the reported TB meets the coals caliber profile for the domestic market which usually ranges between 16,736 and 27,196 kJ/kg [81] based on their HHV. This quality

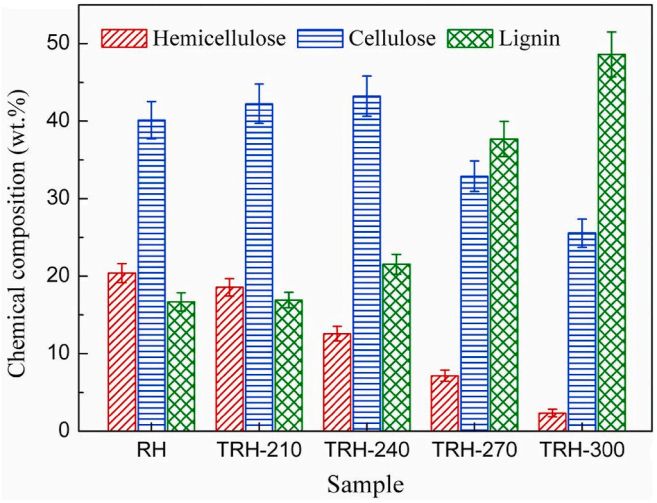

Fig. 1. Chemical composition analysis of raw and torrefied rice husk [110]. Reprinted with approval from Elsevier (License no.: 501798184).

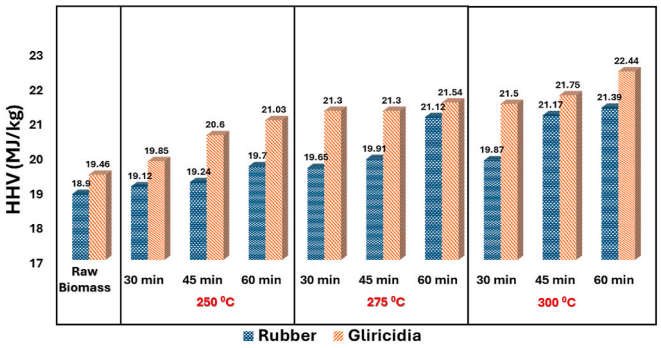

Fig. 2. HHV of raw and torrefied gliricidia and rubber wood at different times and temperatures [65]. Reprinted with approval from Elsevier (License no.: 5502930547429).

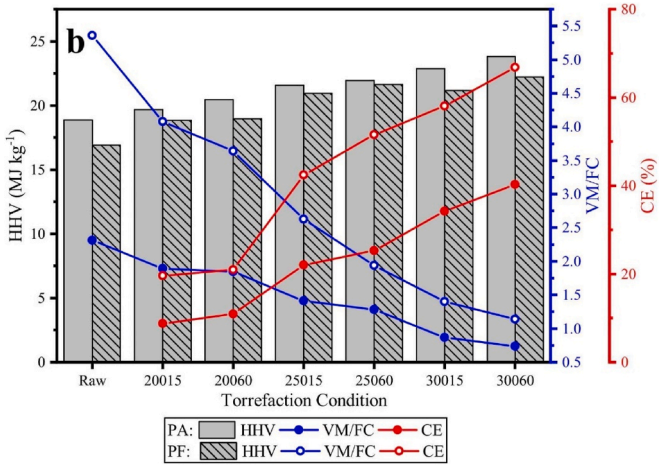

Fig. 3. Correlation between VM and FC, carbon enrichment (CE), and higher heating value (HHV) for crude and torrefied biomass. Passion fruit peel waste (PF) and pineapple peel waste (PA) [74]. Reprinted with approval from Elsevier (License no.: 5502931011634).

can also be corroborated using their low sulfur content as a yardstick to measure the extent of SO_x emission by fuel samples to minimize environmental pollution and climate change. Overall, the hallmark of fuel energy value (HHV) of the TB (16,000–32,100 kJ/kg) is close to most of the coal samples reviewed (16,500–33,000 kJ/kg) as reported in Tables 1 and 2. This is a pointer that most anthracite and high-grade bituminous coal exhibit a better fuel property compared to TB [84].

3. Comparative analysis of the fuel ratio of coal and torrefied biomass

Another important parameter to comparatively determine the disparity and similarity of solid fuel quality is called fuel ratio (FR). It is calculated as the ratio of the FC to the VM, both expressed as percentages [113]. The FR is important because it helps in understanding the combustion characteristics of the fuel. A higher FR indicates a higher proportion of FC, suggesting that the fuel burns more slowly and with greater difficulty, whereas a lower fuel ratio indicates a higher proportion of VM, which means the fuel ignites more easily and burns faster [114,115]. Thus, the fuel ratio can provide insights into the efficiency, environmental impact, and handling requirements of different solid fuels.

Some researchers have explored the influence of FR on the VM and FC of both TB and coal. For instance, Kongto et al. [77] observed that a rise in torrefaction temperature over a longer period decreased VM. In contrast, an elevation in the FC enriched the FR of torrefied rubber wood from 0.22 to 1.23. Also, a higher temperature allowed more hemicellulose and cellulose to decompose, which resulted in a high FR [77]. The torrefied rubber wood FR is in close range with 1.50 recorded for Singrauli India coal [116], and 1.40 recorded for torrefied teak wood [108], but relatively low in comparison to 2.60 recorded for torrefied Melina wood [108] (Table 2).

Adeleke et al. [108] further expounded that a higher FR is a significant indicator of an improved ignitability index for solid fuel. This is consistent with claims about coal, where low FR scores result in a strong and better ignition propensity profile and could lead to accidental ignition of coal during reserve storage. Conversely, high FR scores bring difficulties in coal ignition, resulting in steady and improved combustion operation [116]. Furthermore, Fig. 4 revealed the torrefaction temperature dependency on the FR [62]. However, due to the rich content of VM, the FR of both torrefied *Mangifera indica* seed and *Passiflora edulis* shell was very low compared to that of bituminous coal [117] and Singrauli India coal [118]. Moreover, a torrefied *Passiflora edulis* shell has a higher FR, which implies that it has superior combustibility than a torrefied *Mangifera indica* seed. Notably, it was pragmatically established that there was an upsurge in the FR when the TB was co-fired with bituminous coal as shown by the red dots in Fig. 4 [62]. Figs. 5 and 6 display the time and temperature dependency of the FR of specific raw and torrefied biomass types. A similar scenario was observed for torrefied Ananas comosus peel and Annona squamosa peel [63] and for torrefied *Washingtonia filifera* petiole and *Sterculia foetida* follicle, respectively. However, it was affirmed that the FR of the torrefied *Washingtonia filifera* petiole and *Sterculia foetida* follicle are inferior to the FR of bituminous coal (1.5–2.5) and this does not differ in the case of FR value reported for torrefied Ananas comosus peel and Annona squamosa peel [63].

Rago et al. [120] reported experimental findings on the FR of blended TB (mango branches + waste newspaper). Torrefied mango branches exhibited the highest FR compared to the blended TB, which also exhibited higher FR compared to the waste newspaper as presented in Fig. 7. Nevertheless, the FR of both the torrefied blended and individual TB are far behind that of torrefied *Acacia nilotica* wood [121] and the typical FR of coal (0.5–2.0) use in coal-fired plants [120].

Singh et al. [122] highlighted that fuels with a FR significantly

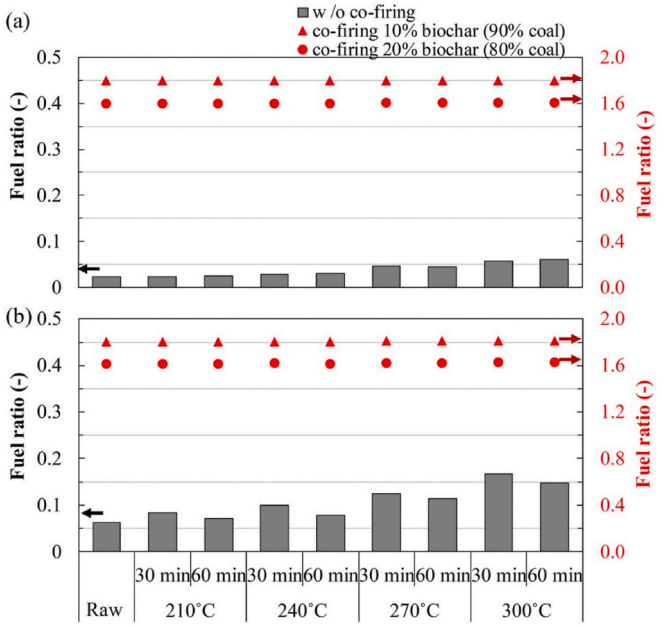

Fig. 4. Time and temperature dependency of FR of (a) raw, and torrefied *Mangifera indica* seed (b) raw and torrefied *Passiflora edulis* shell [62]. Reprinted with approval from Elsevier (License no.: 5502940552240).

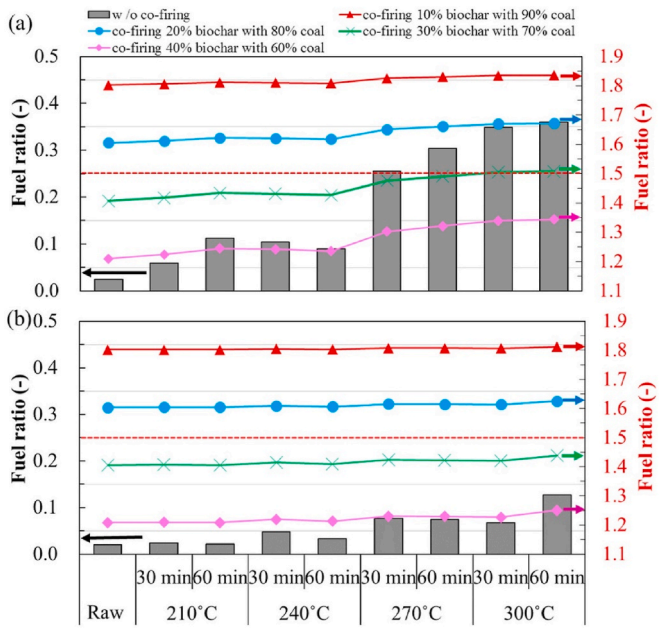

Fig. 5. Time and temperature dependency of FR of (a) raw, and torrefied Ananas comosus peel (b) raw and torrefied Annona squamosa peel [63]. Reprinted with approval from Elsevier (License no.: 5502940859911).

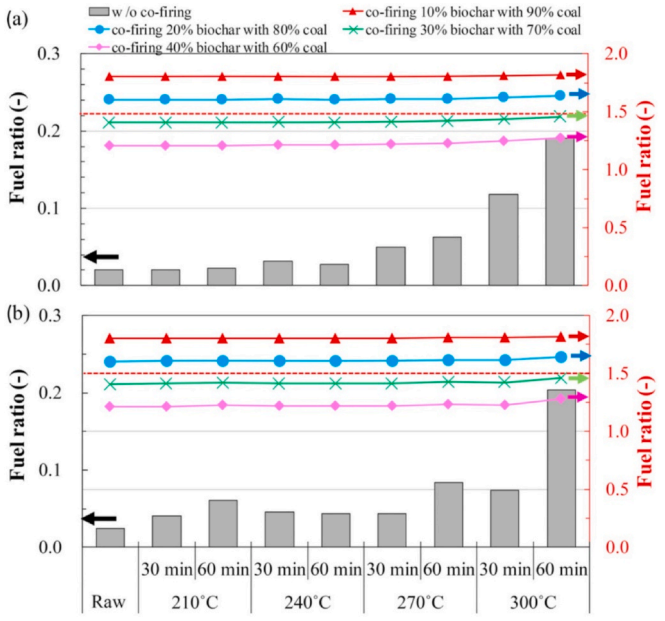

Fig. 6. Time and temperature dependency of FR of (a) raw, and torrefied *Washingtonia filifera* petiole (b) raw and torrefied *Sterculia foetida* follicle [119]. Reprinted with approval from Elsevier (License no.: 5502941104394).

greater than 2 could present challenges in flammability and ignitability during use. This situation could lead to an increase in the unburnt portion of the fuel, thereby reducing boiler efficiency during operation [122]. On the other hand, Rago et al. [120] suggested that biofuels with low FR may still be co-combusted with coal if the FR is mixed within a range of 5 wt%. The FR of torrefied *Hibiscus cannabinus* L. [95] and sugar cane bagasse [75] also falls within the recommended value but is considerably lower than that of Vietnamese anthracite coal [95]. Singh et al. [78] recorded a FR of 1.63 for torrefied *Acacia nilotica* wood and this is somewhat in good agreement with the FR of Zhundong coal (1.86) and this indicates similar chemical properties to the bituminous coal

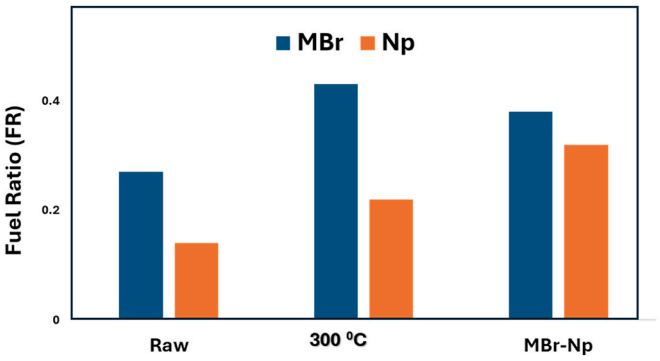

Fig. 7. Comparative FR of individual torrefied mango branches (MBr), waste newspaper (Np), and their blended version (MBr-NP) [120]. Modified with approval from Elsevier (License no.: 5502941416896).

[123]. Similarly, the FR value of 1.75 for torrefied Melina wood [124] was found to be in a very close range with that of Zaoquan bituminous coal which is 1.98 [125]. Moreover, as observed in another torrefaction study, the FR of torrefied *Washingtonia filifera* petiole and *Sterculia foetida* follicle [119], and torrefied pine sawdust [126] are far below the coal standard and possibly will need to be blended with other high FR biomass to bring its FR close to those coals as observed in Table 2. Overall, the FR for majority of TB reported in Table 2 falls closely (with infinitesimal disparity) within the recommended FR value of 0.5–3.0 by Singh et al. [122] for coal use in power plants, boilers, and other applications.

4. Comparative analysis of the ash composition and ash fusion temperatures of coal and torrefied biomass

Comparing the elemental oxide composition and ash fusibility of a solid fuel is essential for evaluating and establishing the combustibility bahavior as well as its profile [6], combustion system configuration [73], slagging [123], corrosion, ash [127] and fouling management [128]. Sher et al. [60] employed ash melting behaviour to evaluate and define the ash fusibility temperatures. It was discovered that following low and medium torrefaction of raw biomass (RB), the initial deformation temperature (IDT) rose, but was still largely behind that of El Cerrejon coal except for softening, hemisphere, and flow temperature that surpasses 1250 °C in comparison to El Cerrejon coal. Thus, the TB is

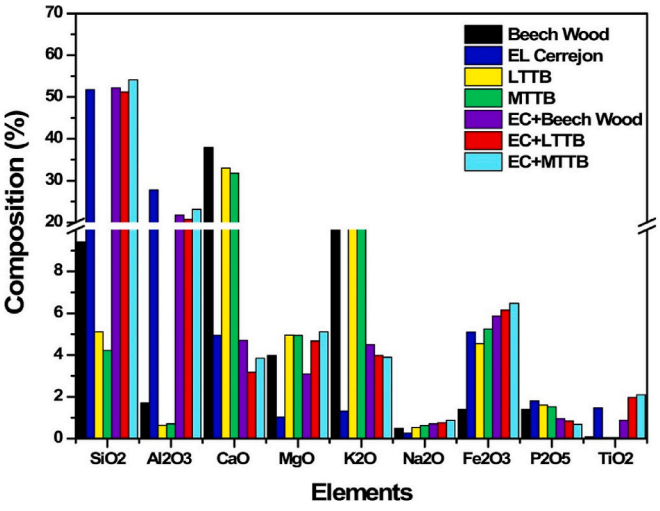

Fig. 8. Comparative ash composition of El cerrejon coal, torrefied beech wood, and their analogue combo in terms of elemental oxides [60]. Reprinted with approval from Elsevier (License no.: 5502950235790).

deemed appropriate for combustion in a fluidized bed combustor. Comparatively from the results presented in Fig. 8, the ash melting property is strongly correlated to ash composition. The ash comprises different alkali and acidic oxides with SiO_2 being the most predominant and TiO_2 being the least. Sher et al. [60] opined that IDT rose owing to the presence of a voluminous amount of CaO, Al_2O_3, Fe_2O_3, and MgO while IDT diminished with K_2O uptick, even though, the high content of potassium in the TB compared to the coal could be problematic during combustion. The ash fusibility and ash content results are somewhat in agreement with the ones reported for torrefied Teak and Melina woods by Adeleke et al. [108], where the ash fusion temperature experiment revealed that the biomass ash melts at −1200 °C. It finally fused at −1300 °C with SiO_2 and TiO_2 being the most predominant. The least of all the elemental oxide compositions discovered in the two TB respectively are as shown in Table 3. This dominance order is in parallel with what was observed for Wudong coal but largely differs from that of Tianchinengyuan and Wucaiwan coal as MgO was predominant in these two coals with the SiO_2 coming behind compared to that of torrefied Teak and Melina woods [83]. Adeleke et al. [108] empirically established that an increase in temperature during torrefaction does not alter the ash content profile nor lower the ash fusibility temperature (especially the IDT) and concluded that the biomass fuels profile met the standard prerequisite for energy production in thermal plants. It was further emphasized that the low volume of TiO_2, Fe_2O_3, and Na_2O may perhaps be responsible for the very low ash fusibility temperature of the TB compared to coal [108]. Comparatively, the ash fusion temperature for both torrefied Teak and Melina woods, as presented in Table 4, are similar to that of sub-bituminous coal and lignite coal [129].

Kongto et al. [77] and Lampropoulos et al. [72] differ in their reports as they observed that SiO_2 was among the least elemental oxides in torrefied rubber wood and olive. It was also affirmed that the torrefied rubber wood's ash components had much more minerals than conventional bituminous, sub-bituminous, and lignite coals. In another study by Doddapaneni et al. [132], SiO_2 was reported to be the highest for torrefied pulp industrial sludge; however, they differ in their fusibility temperature observation as opposed to that of Adeleke et al. [108], because the DT varied between 720 and 770 °C. This can be observed in Fig. 9, which shows the ash fusion temperatures of dried and torrefied pulp sludge. The disparity in the ash melting profile after torrefaction might be ascribed to variations in the biomass inorganic component [132]. Niu et al. [142] that IDT values increase with increasing Al_2O_3 and reduced with the upsurge in K_2O and SiO_2 supported this submission. This finding is consistent with the fusibility reported for Hebei province coal [143]. Liu et al. [143]; however, inferred that ash slagging mainly consisted of SiO_2, the melting point of which was around 1450 °C.

The presence of acidic oxides such as Al_2O_3 and SiO_2 can improve the ash fusion temperature, while alkaline oxides such as CaO and K_2O can reduce the fusion temperature of ash [138]. This resonates with what was suggested by Adeleke et al. [137] that the existence of basic oxides in the coal and bio-coal briquette reduces the softening and melting temperatures of the ashes to 1350 °C. The fusibility temperature of torrefied rubber wood reported by Kongto et al. [77] is very similar to Afşin and Elbistan coal [144] and Guizhou and Yunnan coal [139] which connote that both will have similar ash behavior if used in co-combustion or co-firing operation. However, Oladejo et al. [139] revealed that the ash fusion temperature tends to decrease with an increase in the Silica/Alumina ratio. This can be ascribed to the presence of the amorphous form of SiO_2 and its ability to react with other elements to form silicates with low melting points [139].

Jagodzińska et al. [133] performed ash deposition experiments on torrefied palm kernel shells. The authors reported that higher torrefaction temperature influences fouling and slagging properties. This is because torrefaction slightly decreases ash deposition tendency and affects ash-melting properties. Their study also revealed that the properties of torrefied palm kernel shell is similar to that of coal, especially in terms of IDT, ST, SiO_2, and VM. Nevertheless, there is still a huge disparity in some other elemental oxides like Al_2O_3, Na_2O, and TiO_2 that are present in a very high volume in the polish coal compared to the torrefied palm kernel shell biomass. It should be mentioned that the silica-alumina ratio is a significant indicator of the ash slag formation. It can be observed from the compiled samples in Table 4 that the silica-alumina ratio ranges from 4.92 to 15.62 for the TB ash while it is in the range of 1.37–2.90 for various types of coals. This reveals that the TB ashes reported have higher tendencies of slag formation than coals. This is due to the presence of a large amount of silica compared to alumina. However, some of the TB and coal samples have good silica ratios while others have silica ratios lower than 0.78 which is the range recommended for good coal ash to enable it to fuse [108]. Table 4 also shows that TB ash has a basic/acid oxide ratio (B/A) in the range of 0.11–0.51. This is higher than the B/A ratios of the coal ash reported in previous studies. This indicates that TB has low melting ash, which may not be good for thermal and metallurgical applications. The B/A ratios of some coal ash samples were on the extremely high side (>2). This may be the reason why Adeleke et al. [108] recommended that TB and coal should be agglomerated to improve their ash properties for thermal and metallurgical applications. On a general note, the slagging factor of torrefied biomass is close to the recommended value (<0.6) for coal, which has a low slagging formation. The slagging factor of domestic pellet wood is extremely high. This implied that it has a high formation tendency. This behavior exists in some of the coal ash samples presented in Table 4. Wucaiwan, Tianchinengyuan, and Zhundog coals have high slagging factors. This shows that TB and coal ashes behave similarly while some of these materials are good feedstock for energy generation. This implied that no class of fuel feedstock possesses generalized properties. The high fouling factor presented in Table 4 shows that rubber wood torrefied at different temperatures can pollute the environment or generate foul odors [137]. The fouling factor's low value shows that both coal and TB cause less odour in the environment when used as feedstock in thermal and metallurgical applications. The fusion temperature of torrefied vine pruning [130] is also in a close range with that of lean-grade sub-bituminous coal [137], and bituminous coal [129], but largely differs from that of torrefied wheat straw [134] except for FT which was a bit similar. Adeleke et al. [137] in their research on ash analyses of bio-coal briquettes expatiated that the silica-alumina oxide fraction is an essential parameter that influences the flow properties of coal ash slag. However, it is negatively correlated with DT, ST, and FT [137]. The study also made it clear that the silica oxides ratio is applied to forecast solid fuel ash slagging performance and it showed a positive correlation to DT and FT. It was reported that decent coal must have a great silica ratio ≥0.78, which indicates that it would be difficult to fuse. Furthermore, it was stressed that the proportion of the basic to acidic oxides which have a positive (+) correlation with FT and DT was also considered as an index for slagging behavior.

Fusion temperature (FT) can be used for evaluating silicate-induced slagging, whilst IDT can be used in the evaluation of alkaline-induced slag [145]. The higher the ash melting temperatures, the less severe the ash-induced operation problems become [129]. Holistically, the predominant elemental oxides as per the ash composition is SiO_2 while the TiO_2 is the least in coal and TB. However, a similar general problem associated with the utilization of TB and coal solid fuel remains deposit formation on heater tube surfaces, boiler, and plant walls.

5. Functional group analysis

Fourier transform infrared (FTIR) analysis is usually carried out to explore and obtain detailed information about the structure–activity relationship between the architectural molecular structures [146], functional groups [147], and properties of biomass and coal fuel [148]. In addition, FTIR analysis provides the basis for relating the effect of torrefaction on the functional groups present in the biomass to give researchers fresh thought on how to improve biomass fuel quality as per

Table 3
Elemental oxides in ash and ash fusion temperature of coal and TB.

Fuel sample	T (°C)	Ash composition as per elemental oxides (%)										Fusibility temperature (°C)				References
		SiO_2	Al_2O_3	TiO_2	Fe_2O_3	CaO	MgO	Na_2O	K_2O	SO_3	P_2O_5	DT	ST	HT	FT	
Teak wood	220	30.24	4.84	0.50	3.58	26.80	5.40	3.01	18.26	3.22	4.15	1200	1210	1230	1320	[108]
	240	30.19	5.00	0.41	3.42	26.82	5.45	3.02	18.18	3.23	4.28	1200	1220	1230	1320	
	260	30.22	4.84	0.40	3.62	26.80	5.43	2.99	18.30	3.20	4.20	1200	1220	1230	1320	
	280	30.26	4.82	0.39	3.61	26.70	5.42	2.97	18.46	3.21	4.16	1200	1220	1230	1320	
	300	30.25	4.83	0.39	3.64	26.71	5.42	3.00	18.28	3.20	4.18	1200	1220	1230	1320	
	320	30.34	4.86	0.30	3.60	26.82	5.42	2.86	18.11	3.24	4.07	1210	1220	1230	1320	
Melina wood	220	31.50	4.20	0.48	3.48	26.98	5.22	2.83	18.09	3.22	4.00	1100	1200	1220	1290	
	240	31.68	4.2	0.28	3.28	27.02	5.26	2.86	18.11	3.24	4.07	1120	1200	1210	1300	
	260	31.58	4.23	0.39	3.26	27.01	5.23	2.87	18.12	3.26	4.05	1120	1200	1210	1300	
	280	31.56	4.22	0.40	3.22	27.03	5.21	2.90	18.11	3.27	4.08	1120	1200	1210	1300	
	300	31.49	4.20	0.42	3.21	27.00	5.24	2.91	18.15	3.28	4.10	1120	1200	1210	1300	
	320	31.68	4.20	0.28	3.28	27.02	5.26	2.86	18.11	3.24	4.07	1120	1200	1220	1300	
Yangquan ant.	-	51.25	34.03	1.44	4.57	3.06	0.93	1.05	1.26	0.92	-	-	-	-	-	[125]
Vine prunings	220	-	-	-	-	-	-	-	-	-	-	1,193	-	1,404	1,421	[130]
Shanxi bit.	-	52.02	33.82	2.29	6.01	1.72	0.76	0.65	0.94	0.50	0.15	-	-	-	-	[131]
Pulp industrial sludge	250	42.56	3.77	-	3.01	14.86	1.77	11.14	1.47	-	-	769	1116	1140	1158	[132]
	275	42.42	4.06		3.32	14.77	1.79	11.82	1.58			720	1127	1151	1216	
	300	45.24	4.37		3.08	16.20	1.96	12.72	1.65			733	1125	1142	1229	
Palm kernel shell	600	53.25	3.41	0.17	8.24	22.39	2.31	0.37	5.51	1.64	2.73	1160	1190	-	-	[133]
wheat straw												550	800	950	1300	[134]
Rubber wood	250	3.55	0.255	0.096	3.037	51.99	6.88	0.21	24.46	-	-	>1458	>1458	>1458	>1458	[77]
	300	3.95	0.287	0.146	2.767	51.03	6.99	0.20	25.29							
olive kernel	300	1.26	0.09	0.02	0.283	14.84	2.00	14.41	52.48	2.74	4.46	-	-	-	-	[72]
	500	1.49	0.06	0.04	0.430	16.36	2.24	12.53	57.92	1.31	4.30					
	800	1.38	0.04	0.07	0.897	18.46	2.37	13.25	53.61	1.45	4.35					
Domestic wood pellets	250	12.95	2.63	1.27	3.21	43.95	11.86	2.71	14.52	6.76	0.13	-	-	-	-	[135]
Low-temperature torrefied beech wood	-	5	0.50	00.00	5.00	31.00	5.00	0.50	20.00	-	-0.50	830	1310	1390	1400	[60]
Medium temperature torrefied beech wood	-	4	-0.50	00.00	-5.00	-30.00	5.00	0.50	20.00	-	-0.50	840	1350	-	1370	
EI Cerrejon bit	-	52	27	1.00	5.00	5.00	0.50	0.50	0.50	-	0.50	1240	1260	1270	1290	
Shenmu coal	-	34.06	14.94	0.38	16.95	27.62	1.88	0.22	3.08	0.97	0.28	1062	1121	1186	1237	[136]
j Subbit.	400	58.00	19.97	1.26	8.26	2.56	2.07	0.21	2.04	-	-	1250	1290	1300	1350	[137]
Jincheng ant.		54.19	27.91	0.97	4.23	4.87	1.08	1.89	1.84	2.09	0.25					[138]
Guizhou coal		38.80	13.20	2.30	10.60	21.30	-	3.20	1.50	9.00	-	1349	1360	1382	1418	[139]
Yunnan coal		36.20	14.40	3.70	6.90	25.20	-	2.00	1.10	10.50		1317	1355	1364	1415	[139]
Zhundong coal	-	23.00	11.00	0.70	7.50	26.60	5.70	6.10	0.67	17.00	0.24	-	-	-	-	[123]
Xinjiang Naomaohu coal	-	24.46	17.89	0.93	13.47	24.61	1.21	3.09	1.01	11.31	0.18	1086	1115	1130	1140	[140]
Wucaiwan coal	-	14.08	7.34	0.42	6.28	23.01	28.17	11.62	0.34	8.65	-	-	-	-	-	[83]
Tianchinengyuan coal	-	17.28	9.29	0.70	4.08	8.46	32.23	12.71	0.17	14.98	-	-	-	-	-	
Wudong coal	-	40.67	16.47	0.56	4.66	3.27	29.08	1.16	1.04	2.90	-	-	-	-	-	
Bit												1251	-	1404	1423	[129]
Sub-bit												1218	-	1365	1389	
Lig												1147	-	1261	1286	
Polish coal	815	54.3	24.70	0.86	9.81	1.93	1.35	2.44	2.36	0.79	0.18	1200	1270	-	-	[133]

Where; DT = initial deformation temperature, ST = softening temperature, HT = hemispherical temperature, and FT = final fusion temperature.

Table 4
Oxide ratios of various coals and torrefied biomass at different temperatures.

Fuel sample	TT (°C)	Oxide ratios					
		Silica/Alumina	Silica ratio	Basic/Acid ratio	Slagging Factor	Fouling Factor	Reference
Teak wood	220	6.25	0.46	1.60	0.52	0.34	[108]
	240	6.04	0.46	1.60	0.52	0.34	[108]
	260	6.24	0.46	1.61	0.52	0.34	[108]
	280	6.28	0.46	1.61	0.52	0.35	[108]
	300	6.26	0.46	1.61	0.51	0.34	[108]
	320	6.24	0.47	1.60	0.52	0.34	[108]
Melina wood	220	7.50	0.47	1.56	0.50	0.33	[108]
	240	7.54	0.47	1.56	0.51	0.33	[108]
	260	7.47	0.47	1.56	0.51	0.33	[108]
	280	7.48	0.47	1.56	0.51	0.33	[108]
	300	7.50	0.47	1.56	0.51	0.33	[108]
	320	7.54	0.86	1.56	0.51	0.33	[108]
	275	10.45	0.68	0.72	–	0.10	[108]
	300	10.35	0.82	0.72	–	0.10	[108]
Palm kernel shell	600	15.62	0.81	0.68	0.11	0.04	[133]
Rubber wood	250	13.92	0.06	–	–	5.48	[77]
	300	13.76	0.07	–	–	5.02	[77]
Domestic wood pellets		4.92		4.53	3.06	0.78	[135]
EI Cerrejon bit	–	1.93	0.20	0.13	–	–	[83]
Wucaiwan coal	–	1.92	0.28	3.18	2.75	0.38	[83]
Tianchinengyuan coal	–	1.86	0.52	2.11	3.17	0.27	[83]
Wudong coal	–	2.47	0.18	0.68	0.20	0.01	[83]
Polish coal		2.20		0.22	0.02	0.01	[133]
Shenmu bit	–	2.28	0.84	1.01	0.10	0.03	[140]
Jincheng ant		1.94	–	0.17	0.03	0.01	[138]
L Sub-bit		2.90	0.37	0.19	–	0.00	[137]
Zhundong sub	–	2.09	0.38	1.34	2.28	0.09	[123]
Xinjiang Naomaohu coal	–	1.37	0.62	1.00	1.13	0.04	[141]
Yangquan ant	–	1.51	0.86	0.13	0.01	–	[125]
Shanxi lv bit	–	1.54	0.68	0.11	0.01	–	[131]

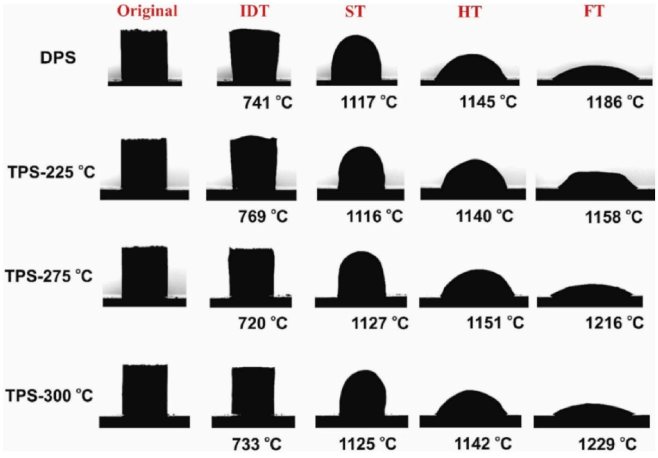

Fig. 9. Ash fusion temperatures of dried and torrefied pulp sludge [132]. (Open access, which permits unrestricted use).

combustibility, grindability, fusibility, and flammability [103]. Table 5 presents the various architectural functional groups and the corresponding wave number ranges. There is no significant difference in the functional groups present in TB as against that of coal as displayed in examples of FTIR spectral as shown in Figs. 10 and 11 for different TB from *Acacia nilotica* [78], canola residues [73], mustard crop residue [149], and yard waste [150]; and different coals from different coal mines in China [151,152], and bituminous coal [136]. For instance, in Fig. 10(A), the FTIR of five different coals from Daxing (DX), Shuangliu (SL), Sijiazhuang (SJZ), Yangliu (YL), and Wolonghu (WLH) were juxtaposed [151]. While there is a slight difference in peak intensity, most of the peak locations were similar, indicating a similarity in functional groups among the coal samples. Similar observations were reported in Fig. 10(B) for four bituminous coals from Gansu, Shanxi,

Table 5
Common architectural functional groups and essential corresponding characteristic absorption bands of FTIR spectra in both TB and coal [147,148].

Functional group assignment	Wavenumber range (cm^{-1})
Free OH	3685–3600
OH self-contained hydrogen bond	3600–3500
OH stretching vibration in phenol, alcohol, carboxylic, peroxide, moisture	3550–3200
CH_3 asymmetric stretching vibration	2975–2950
CH_2 asymmetric stretching vibration	2935–2915
CH_3 symmetric stretching vibration	2875–2860
CH_2 symmetric stretching vibration	2860–2840
Aliphatic C═O stretching vibration	1720–1800
Aromatic C═O stretching vibration	1715–1660
Aromatic C═C stretching vibration	1615–1585
CH_2 asymmetric deformation vibration	1480–1465
CH_3 asymmetric deformation vibration	1460–1435
CH3 symmetric bending vibration	1385–1370
C–*O*–C stretching vibration	1160–1120
Aromatic nucleus (CH), adjacent H deformation	900–730
n-Alkane side chain skeleton $(CH_2)_n$ vibration	740–716
OH in carboxylic acids	979–921
COOH	1715–1690
Phenolic deformation C–*O*–C (stretching)	1300–1000

Anhui and Inner Mongolia [148]. In contrast, Fig. 10(C) compared the FTIR analysis of dried raw *Acacia nilotica* (DAN), and torrefied *Acacia nilotica* wood at different temperatures and times (TAN) [78]. The FTIR results revealed that torrefaction alters the chemical structure of biomass, mainly through the breakdown of hemicellulose, affecting hydroxyl group interactions and enhancing biomass durability and storability by modifying bond intensities and cleaving chemical groups. Similarly, Fig. 10 (D) compares the FTIR results of RB and TB of canola residue at different temperatures and times [73]. Torrefaction significantly modifies the surface functional groups of canola residue, reducing and shifting oxygen-containing group peaks as observed in FTIR spectra,

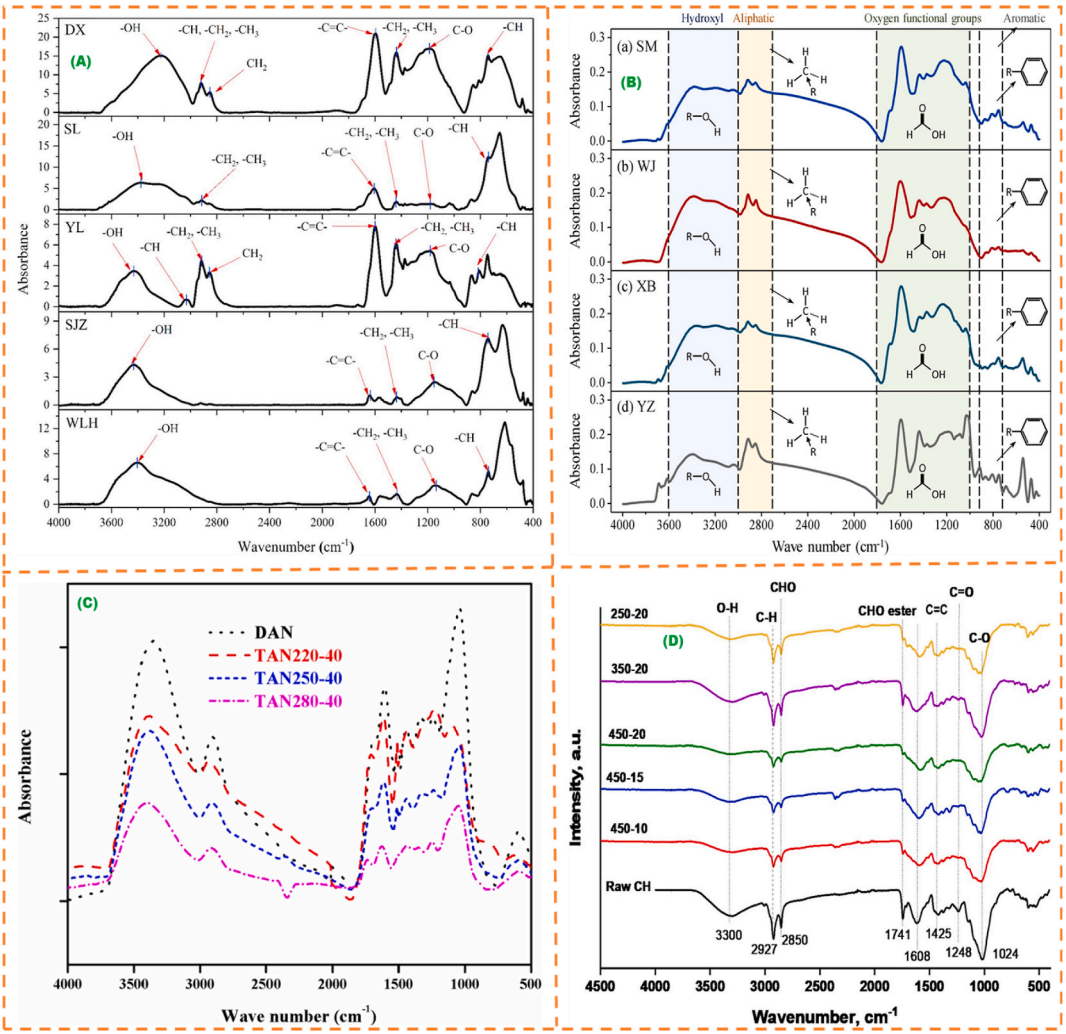

Fig. 10. FTIR spectra of: (A) Five different coals from Daxing (DX), Shuangliu (SL), Sijiazhuang (SJZ), Yangliu (YL), and Wolonghu (WLH) [151], (B) Four bituminous coals from Gansu, Shanxi, Anhui and Inner Mongolia [148], (C) Dried raw (DAN), and torrefied *Acacia nilotica* wood at different temperature and time (TAN) [78], (D) RB and TB of canola residue at different temperature and time [73]. Reprinted with approval from Elsevier (License no.: 5502951221204, 5502960343249, 5502960576516 and open access respectively).

highlighting microwave power as crucial in decomposing lignocellulosic structures and removing oxygen groups. The presence of O–H stretching diminishes with torrefaction intensity, indicating moisture loss and dehydroxylation, especially noticeable at higher torrefaction conditions like 450 W for 20 min, while peaks around 2918–2932 cm^{-1} show C–H stretching in various organic groups [73]. The absorption band for functional groups present in the TB and coal fuel matrix as observed in Figs. 10 and 11 are in the same range as presented in Table 5. However, the peak intensities of the spectra are not the same.

Fig. 11 (A) compares the FTIR analysis of raw, and torrefied mustard crop residue (MCR) at different temperatures and times [149]. The figure shows that MCR (microcrystalline cellulose) retains similar oxygen-containing functional groups at 200 °C for 30 min, suggesting organic content stability at this temperature. However, above 250 °C, significant thermal decomposition of organic groups, especially hemicellulose, leads to a noticeable reduction in the absorption peaks of these groups. The broader O–H band indicates the presence of hydrogen bonds in cellulose and hemicellulose, with the bound moisture and water removed during torrefaction, evident from the decreased OH peak intensity between 3400 and 3200 cm^{-1}. The C–H peak reduction reflects the loss of methyl and methylene groups, while the decrease in the C═O peak signifies the breakdown of carboxyl groups, leading to less oxygenated compounds and gases like CO and CO_2, simplifying MCR's organic composition and reducing its oxygen content [149]. Jaideep et al. [150] also compared the FTIR analysis of raw and Nitrogen-torrefied yard waste as shown in Fig. 11 (B). A distinct peak at 3693 cm^{-1}, unique to raw biomass and indicative of O–H stretching in alcohols, disappears in torrefied samples, suggesting alcohol groups, along with moisture, are lost at temperatures starting from 170 °C [150]. The broad peak between 3600 and 3200 cm^{-1}, representing O–H stretching in hydroxyl groups associated with moisture, alcohols, phenols, and organic acids—characteristics of crystalline cellulose and hemicellulose—decreases with rising torrefaction temperatures. This reduction, due to dehydration reactions that destroy hydroxyl groups and form non-polar unsaturated structures, diminishes this peak and increases the material's hydrophobicity as the temperature increases.

Similar observations were reported by Saher et al. [60]. The authors compared the FTIR analysis of RB and TB of beech wood (Low and medium temperature (LTTB and MTTB)) as shown in Fig. 12 (A) [60]. More specifically, during torrefaction, cross-linking structures are degraded by breaking H-bonds and dissolving part of functional moieties containing OH and O_2 groups, and this promotes the release of aromatic functional architectural moieties. The destruction of the OH group during torrefaction leads to the formation of non-polar unsaturated structures, a significant reduction in moisture content, and an increase in the hydrophobicity of the TB. Thus, these spur its combustibility and

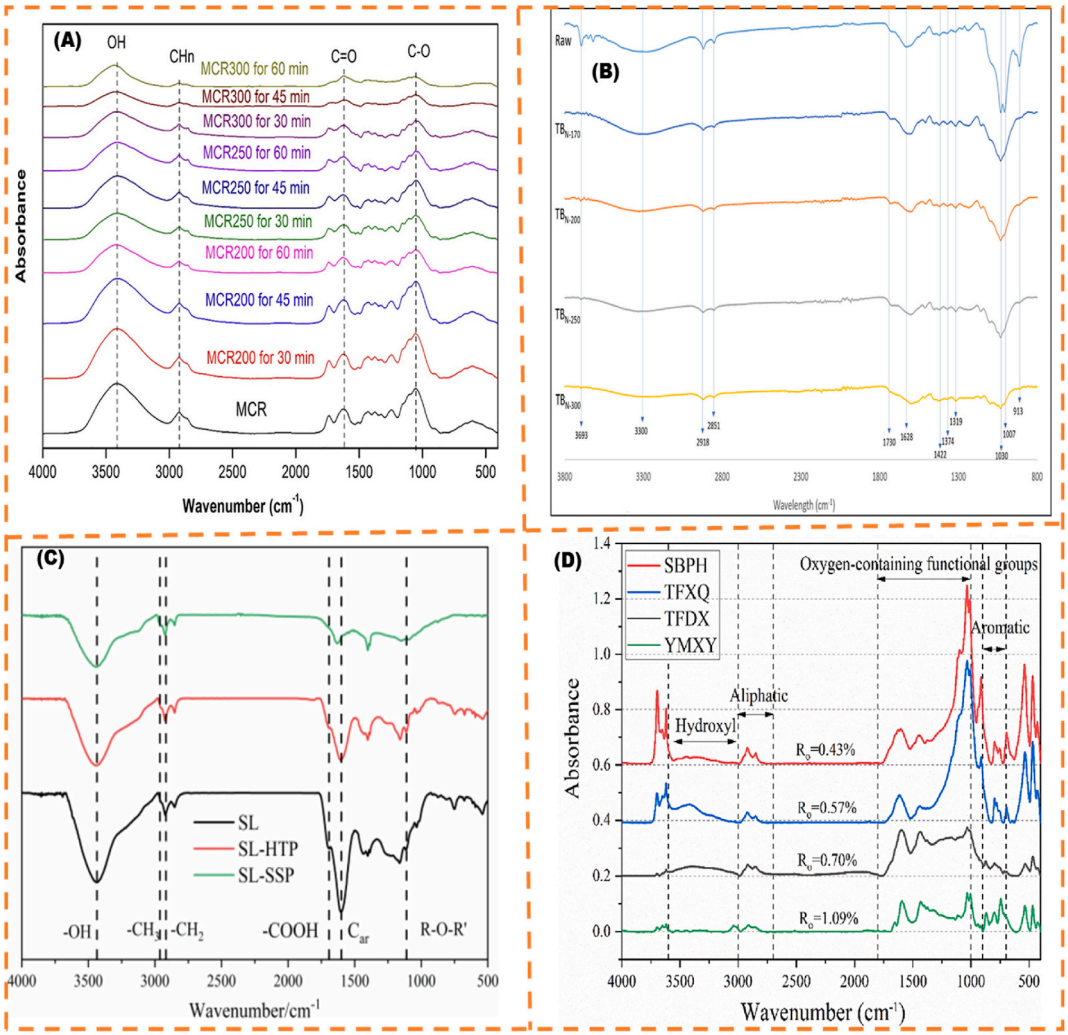

Fig. 11. FTIR spectra of: (A) Raw, and torrefied mustard crop residue (MCR) at different temperatures and times [149], (B) Raw and Nitrogen-torrefied yard waste [150], (C) Shengli lignite coal (As-collected (SL) and pretreated (SL-HTP and SL-SSP)) [91], (D) Five bituminous coals from Daxing (TFXQ), Xiaoqing (TFDX), Puhe (SBPH) and Xinyi (YMXY) [147]. Reprinted with approval from Elsevier (License no.: 5502961157731, 230306013522, 5502971305281, and 5502980034356 respectively).

flammability to the same level as coal [153]. It has been shown that H-bonds in solid fuel are predominantly self-associated OH and OH-ether H-bonds [147]. The OH-ether hydrogen content largely decreases, showing that the H-bond morphology in fuel metamorphosed after heat treatment or torrefaction, and some cross-linking H-bonds with O_2 are demolished [91]. This is because hydrophilic functional architectural groups, such as OH, in the solid fuel are eliminated during the torrefaction or pretreatment operation as reported for some TB fuels such assugarcane bagasse [75], avocado, mango, and Lychee seeds [66], and patula pine [79].

During torrefaction, the thermal stability of hemicellulose present in passion fruit peel and pineapple peel waste becomes weaker [74]. This was linked to the destruction of chemical bonds in the hemicellulose group which then led to the ejection of hydrocarbons comprising C–O and C–H functional groups and thus afforded TB with an energetic profile analogous to peat and lignite coal [74]. This agrees with the claim that torrefied rubber wood has more C–C and C–H bonds, and the capacity of these bonds to generate energy is superior to that of the O–H and C–O bonds in the raw rubber wood [77]. In addition, negligibility in the intensity of the C–H peak in TB is a sign of a reduction in VM volume [72]. Also, as the torrefaction temperature increases, the intensity of the absorbance peaks from all chemical functional groups become weaker due to an upsurge in weak intra- and inter-molecular hydrogen bonds. This shows the thermal degradation of lignin, hemicellulose, and cellulose [72]. A study stated that as the torrefaction temperature increased, marked alterations in the fingerprint region were detected as the C–C, C–O, and C–H bonds were altered owing to the decomposition of spent coffee grounds [69]. It was further explained that the C═O peaks are linked to carboxylic acid, aldehyde, and ketone that are generated following the putrefaction of cellulose and hemicellulose components present in biomass [60].

Singh et al. [78] reported that with a rise in temperature during torrefaction, the intensity of peaks reaffirmed the rupture of chemical bonds such as C═O, C–O–C, and C–H–O that are present in the biomass. It was further observed that a fall in peak intensity may be attributed to the ester group attached to the hemicellulose being cleaved by a deacetylation reaction. The study concluded that the breakdown of hemicellulose during torrefaction is mainly accountable for the alteration in the chemical structure of RB [78]. This observation is not different from those reported by previous studies [73,154]. In addition, Patidar et al. [149] stated that the intensity of the OH peak decreases with the degree of torrefaction due to the removal of bound moisture and water through a dehydroxylation reaction. It was also pointed out that absorption of the C–O peak diminished due to the occurrence of reactions like depolymerization, cyclic C–O, decarboxylation, and ring rupture [73]. Subsequently, it leads to the materialization of a series of

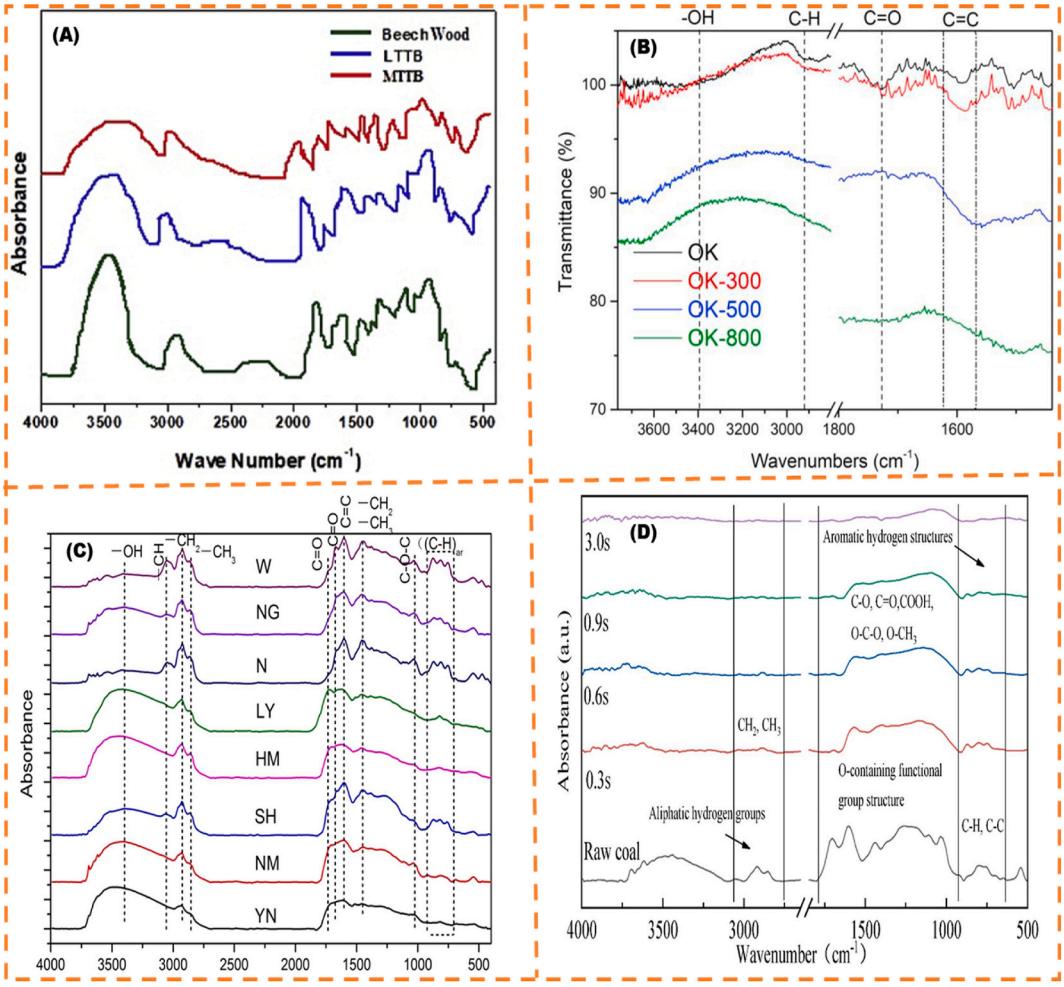

Fig. 12. FTIR spectra of: (A) RB and TB of beech wood (Low and medium temperature (LTTB and MTTB)) [60] (B) RB and TB of olive kernel [72], (C) Eight coals of low-medium rank [152], (D) Shenhua bituminous coal [136]. Reprinted with approval from Elsevier (License no.: 5502980564507, 5502980957025, 5502981185396, and 5502990014950 respectively).

less oxygenated compounds (e.g. alcohols, ethers, aldehydes, and acids) and non-condensable gases like CO and CO_2 [154]. The little disparity in the absorbance peak intensity might also be due to mining and cultivation locality, soil and meteorological conditions, biomass species, processing conditions, torrefaction approach, and or refining strategy [154].

6. Hydrophobicity property

Hydrophobicity refers to the propensity of non-polar molecules (or part of molecules) to be aggregated in water. The contents of hemicellulose, cellulose, and lignin of a biomass fuel play important roles in the hydrophobicity properties [142,155]. Of these three components, hemicellulose has the greatest capacity for water sorption, while lignin has the least. Enhanced hydrophobicity makes it easier to store biomass outdoors for extended periods without being affected by the raw material's hydrophilic behavior or biological degradation [142]. For a biomass to be torrefied means that the biomass has been pyrolyzed under relatively mild conditions at reaction temperatures between 200 and 300 °C for about 1 h in inert or oxygen-reduced environmental conditions [155,156]. Biomass components such as hemicellulose, cellulose, and lignin usually undergo degradation around this temperature range. However, hemicellulose mainly degrades via depolymerization as well as bond cleavage in the corresponding amorphous region [155]. Hence, TB crystallinity increase is dependent on the conditions of torrefaction [157]. Due to the elimination of the hydroxyl group during torrefaction, the hydrophobicity of the TB biomass improves.

Law et al. [158], stated that it is scientifically correct that a surface is hydrophobic when its static water contact angle (Θ) is greater than 90°. Unlike RB, higher calorific values, lower moisture content, lower atomic O/C and H/C ratios, higher grindability, lower hygroscopicity, and more uniform properties have been reported for TB [153]. Biomass absorbs moisture into the cell walls by the OH group's attraction, which holds H_2O molecules via H-bonding. Hence, biomass is hygroscopic. However, hydroxyl groups are partly destroyed during the torrefaction process of biomass because of this; dehydration and hydrogen bond formation are inhibited. Therefore, after torrefaction, hygroscopic biomass is known to be hydrophobic [159]. More so, the equilibrium moisture content (EMC) is significantly reduced in the biomass [160]. Several reactions occur in biomass at different temperature regimes [161]. These reactions include dehydration, devolatilization, and carbonization of hemicellulose, depolymerization and devolatilization/softening of lignin; and depolymerization devolatilization of cellulose. The physical properties, chemical composition, and energy content of the biomass are significantly affected because of these reactions. Therefore, a solid uniform product with high-energy content and lower moisture composition is produced after the torrefaction operation. The storage stability of biomass is improved owing to the loss of hydrophilic bonds during torrefaction operation; hence, TB is more hydrophobic. There is partial destruction of the OH groups in the biomass during the torrefaction

process through dehydration, leading to the prevention of H-bond formation. This results in the hydrophobic profile of TB which makes it less vulnerable to degradation during stockpiling. Tumuluru et al. [161] and Adeleke et al. [162] reported that dry matter losses during stockpiling are marginal. Chen et al. [153] studied the hygroscopic nature of fir (a softwood species), which is a biomass that when pretreated by torrefaction. The study revealed that EMC of the TB was reduced by 35 % or more in comparison to the EMC of RB. When the torrefaction temperature increased, this implied a lower water absorption behaviour of the TB. In addition, the uptick in the torrefaction temperature increased the contact angle of the torrefied wood surface in the range of 103–113 °C, corresponding to a hydrophobic surface (>90°). Tumuluru et al. [161] when untreated biomass pellets and treated biomass pellets at different temperatures of 200 and 240 °C were plunged in water for about 1 h. However, during the first 10 min of immersion, the untreated biomass pellets disintegrated inside the water while there was total dispersion of the untreated biomass in water at the end of 1 h. The torrefied (at 200 °C) pellets were found to maintain their original profile for the first 10 min of water immersion, however, there was some degradation after 1 h. Meanwhile, torrefied (at 240 °C) pellets showed no sign of disintegration in water for about 1 h. As a result, the degree of integration of biomass pellets is decreased when torrefaction temperature increases. The hydrophobicity of biomass pellets is improved owing to the increase in the treatment severity.

In a related study by Wang et al. [92] the impact of the torrefaction process was investigated on the profile of pellets obtained from woody biomass of spruce stem wood, barks, and forest residues. The torrefaction temperature range utilized was between 225 and 275 °C under two residence times of 30 and 60 min. Hydrophobicity of the biomass was studied, in relation to water uptake capacity or water resistance of the raw and torrefied pellets. The test was carried out by immersing both the raw and torrefied pellets into the water for a certain period of testing. The raw wood and forest residue pellets disintegrated within a short period when immersed in water. Pellets produced from barks retained good stability formation. However, the structural integrity was lost after about 4 h of water immersion experiment. The higher hydrophobic extractive contents of the bark pellets were the reason for the higher water resistance compared to other pellets. It was reported that the torrefied pellets showed low water uptake capacity with retained intact structure after the period of testing compared to the raw pellets. The study further established that the rise of torrefaction severity significantly improves the hydrophobicity of the pellets having strong resistance to water sorption with structural integrity being maintained after the immersion [92].

Zhang et al. [163] studied the impacts of the variation of torrefaction temperature (200–350 °C) on the hydrophobicity of soybean straw pellets (SSP) and pine wood pellets (PWP). The EMC and water resistance methods were used to evaluate the hydrophobicity of the pellets. A better hydrophobicity is related to lower EMC and water resistance of the sample under consideration. The investigation compared the hydrophobic properties of SSP and PWP at both the raw and torrefied states. With the torrefaction temperature increasing, the EMC of the torrefied pellets decreased. It was reported that pellets of both the soybean straw and pinewood at a torrefied temperature of 350 °C revealed that the pellets are highly hydrophobic. This makes them suitable for storage without any special threat of deterioration biologically. More so, due to the low water content to transport with the biomass, the cost of transportation of the TB was reduced compared to the cost of transporting the raw pellets [163].

Aside from the presence of water in pellets which significantly influenced the hydrophobicity, the biomass chemical composition also greatly affects the hydrophobic characteristics of the pellets. Torrefied pellets have a lower affinity for water because the hemicellulose of torrefied pellets is known to reduce significantly because of volatilization and carbonization during torrefaction operation [164]. Hence, hemicellulose loss leading to slight lignin content refinement implies that there would be a reduction in the H-bonding activities in the torrefied pellets [165]. PWP showed better water resistance than SSP. The rationale behind strength against water absorption is better explained using the hydrophobic behaviour of torrefied pellets. For this reason, having good hydrophobicity and water resistance for high-temperature torrefied pellets are good pointers to being able to be stored outdoors. Djyakon et al. [166] investigated the impact of torrefaction temperature on the hydrophobic properties of waste biomass derived from food processing. The food processing wastes utilized in the study included black currant pomace, orange peels, apple pomace, pumpkin seeds, and walnut shells. The torrefaction operation was done between 200 and 300 °C at 20 °C stepwise. The determination of the hydrophobic properties of the waste biomass involved using the water drop penetration time (WDPT) method of analysis. The hydrophobicity values of the TB were compared with that of RB dried at 105 °C. The study reported that even the most hydrophilic samples (apple pomace and black currant pomace) reached an extremely hydrophobic state at a temperature of 300 °C. However, other samples such as walnut shells, orange peels, and pumpkin seeds were severely hydrophobic at 220 °C with a time of penetration that was over 1000 s. Extreme hydrophobic properties were reached at 260 °C for walnut shells, orange peels, and pumpkin seeds. This further reinforced the established knowledge that the biomass torrefaction process enhanced its hydrophobic profile. The uptick in the temperature of the torrefaction operation makes the moisture absorption resistance to be improved. Dyjakon et al. [66] examined the hydrophobicity of forestry biomass residues such as Horse chestnuts, Oak acorns, and spruce cones through torrefaction.

A water drop penetration time test was employed in the determination of the hydrophobic properties [167–169]. The test was used for forestry residues (Horse chestnuts, oak acorns, and spruce cones) [170], rubberwood pellets [171], and coffee husk (CH) and spent coffee ground (SCG) [172]. It is important to note that any biomass that reaches the value over 3600 s time is acknowledged to be extremely hydrophobic. The forestry biomasses were observed to be extremely hydrophobic at different torrefaction temperatures. Kanwal et al. [94] characterized the physicochemical properties of torrefied corncob at different temperatures of 200, 225, 250, 275, and 300 °C at different residence times of 15, 30, 45, and 60 min. The properties obtained were compared with that of Thar coal. The hydrophobicity of the torrefied corn cob was optimum at 300 °C torrefaction temperature and at 60 min residence time. This further affirms that as torrefaction temperature and residence time increase, the affinity of biomass to absorb water is lowered. More so, at these maximum temperatures and residence times for torrefying the corn cob, the properties were found to be comparable with that of Thar coal.

Based on findings by several scientists on biomass, the hydrophobicity values of some biomass materials based on their EMC values are presented in Table 6. It can be observed from the presented Table 6 that the hydrophobicity value of the RB was higher than the TB. This implied that the RB is hydrophilic; however, when subjected to torrefaction temperatures, there was breakdown of the water molecules in the biomass due to dehydration, devolatilization, and carbonization of hemicellulose; depolymerization and devolatilization/softening of lignin; and depolymerization devolatilization of cellulose. As the torrefaction temperature increases, the hydrophobic property of the biomass improves for proper storage over a long period without disintegration.

7. Grindability property

Grindability is a parameter that best depicts the resistance of a material to size reduction. The ratio of energy used in a fragmentation process to the resultant outcome, such as cumulative retained mass or volume in a given mesh, increased surface area of the milled particles, or an increase in product finer fractions, is known as the grindability of materials. It is one of the important parameters for determining the performance of the torrefied biomass. Particle size distribution

Table 6
Biomass type and EMC values.

S/N	Biomass type	EMC value (%)	Ref.
1.	DCS (raw)	10.8	[160]
	TCS at 200 °*C*	7.1	
	TCS at 250 °*C*	5.6	
	TCS at 280 °*C*	4.3	
2.	Fir (Raw)	5.49	[50]
	Fir at 200 °*C*	3.60	
	Fir at 210 °*C*	3.34	
	Fir at 220 °*C*	3.07	
	Fir at 230 °*C*	2.34	
3.	SSP (Raw)	9.5	[163]
	SSP at 200 °*C*	8.2	
	SSP at 250 °*C*	7.4	
	SSP at 300 °*C*	5.5	
	SSP at 350 °*C*	4.6	
4.	PWP (Raw)	9.7	[163]
	PWP at 200 °*C*	6.8	
	PWP at 250 °*C*	4.5	
	PWP at 300 °*C*	4.3	
	PWP at 350 °*C*	2.9	
5.	CPS (Raw)	12.5	[173]
	CPS at 200 °*C*	9.0	
	CPS at 250 °*C*	5.0	
	CPS at 300 °*C*	4.5	
6.	Leucaena (Raw)	6.2	[169]
	Torrefied Leucaena	5.8	
	EFB (Raw)	8.0	
	Torrefied EFB	7.0	
7.	LTM (Raw)	8.23	[174]
	20 % HTM-LTM (10 % MC)	8.66	
	20 % HTM-LTM (14 % MC)	7.91	
	20 % HTM-LTM (16 % MC)	7.26	
8.	Australian pelletized wood at 300 °*C*	14.0	[175]
9.	Loblolly pine (LP) at 250 °*C*	10.5	[142]
	LP at 275 °*C*	8.5	
	LP at 300 °*C*	8.3	
10.	Kenaf (Raw)	16.71	[176]
	Kenaf at 200 °*C*	14.44	
	Kenaf at 230 °*C*	13.46	
	Kenaf at 250 °*C*	12.49	
	Kenaf at 280 °*C*	12.13	
	Kenaf at 300 °*C*	11.65	
11.	Wood pellet (WP) (Raw)	10.86	[176]
	WP at 200 °*C*	10.51	
	WP at 230 °*C*	8.89	
	WP at 250 °*C*	7.71	
	WP at 280 °*C*	6.78	
	WP at 300 °*C*	6.27	

- DCS (Dried Cotton Stalk), TCS (Torrefied Cotton Stalk), SSP (Soyabean Straw pellet), PWP (Pine Wood Pellet), CPS (Cocoa Pod Shell), LTM (Lightly Torrefied Material), HTM (Highly Torrefied Material), MC (Moisture Content).

predictability is essential for grindability properties, which are crucial for the preparation of solid biofuel for energy conversion processes. In addition to causing feeding issues, unburned fuel may pass through the conversion process due to particles with an excessively large or wide distribution [177,142].

The hardgrove grindability index (HGI) is used to define the grindability index of brittle materials such as coal [178]. However, biomass has a fibrous anisotropic nature that limits the direct application of HGI. Thus, the HGI has been modified to suit TB. The modified hardgrove grindability index (mGHI), resistance to impact milling, hybrid work index, ISO grindability, and specific grinding energy have become widely known indices to check for the grindability of biomass in its raw, torrefied, and pelletized forms [179]. Manouchehrinejad et al. [178] proposed the use of a volumetric hardgrove grindability index to evaluate the grindability of bulk materials like RB and TB. For biomass upgradation for post-application, the volumetric hardgrove grindability index (HGI) is a very important factor. In the estimation of energy usage, capacity, and mill performance as well as the particle distribution after the milling process, the HGI test is the most used. It is generally known that a higher HGI value is an indication that the solid fuel can be ground effortlessly to give higher mill outputs with lower power inputs. Having a well-informed understanding of the grindability profile of a TB is a relevant criteria for their utilization. There is rupturing of the structures of the cell wall after torrefaction and bigger pores development, bringing significant collapse of the cell walls [50]. The release of VM in the form of gases and liquid condensation during torrefaction causes the cell walls to collapse [79]. The destruction of the cell walls makes the TB to be convenient to grind, thereby improving the grindability. Hence, there should be improvement in grindability for efficient fuel application [59]. It can be stated specifically that if biomass is pulverized into small particles, the better the grindability of the biomass material, and more energy is saved [178].

Dyjakon et al. [180] investigated the grinding energy demands of the different biomass (Sunflower husk, Beetroot pomace, Grass, Pine tree, and wheat straw). The energy required for grinding ranged between 16.28 kJ/kg and 130.72 kJ/kg for the untreated and TB pellets at 200 and 300 °C. The sunflower husk pellets and the beetroot pomace pellets produced the lowest and highest energy demand for grinding, respectively. A relationship between grindability and mechanical durability was established to ensure that the most durable pellets would require the highest grinding energy and vice-versa. More specifically, the torrefaction temperature applied had an impact on the grindability of the biomass. A further explanation suggests that grindability as well as mechanical durability have a close relation to the natural fibers such as hemicellulose, cellulose, and lignin content in the biomass. The hemicellulose natural fiber decomposes when torrefaction or thermal treatment is above 200 °C [181]. Jiang et al. [151] studied the influence of torrefaction temperature and holding time on the grindability of four torrefied biomasses which include two agricultural biomasses (corn straw and wheat straw) and two forestry biomass (polar wood and cedar wood). The grindability of the torrefied biomass significantly improved owing to the grindability of straw biomass at higher temperatures compared to woody biomass which showed different effects. By comparing the coefficients of decomposition of the straw biomass and woody biomass, the hemicellulose and cellulose in the straw torrefied biomass are substantially decomposed at 300 °C. Yu et al. [182] torrefied wood pellets obtained from the Yeongdong plant in a batch-type fixed bed reactor. Among several properties explored was the grindability which was known to improve through the torrefaction process because of the fibrous structure degradation [183]. The thermally treated biomass grindability index (TTBGI) method was used to determine the grindability. Various TTBGI values for both raw and torrefied pellets were obtained. Generally, there was almost a linear relationship between the degree of torrefaction and the enhancement in the grindability of the torrefied wood pellets. Improvement in the grindability of biomass is directly proportional to the torrefaction temperature [182]. More so, it is important to determine the grindability index of coal for better classification. These classifications are usually based on the HGI values that are presented in Table 7. Coals are majorly used as fuel in the combustion chamber of power plants. The coal requirement values for utilization in power plants should have an HGI greater than 60 (HGI >60) [180]. The grindability value of 100 HGI was recommended to be a reference standard [184].

It is important to state that coals having the highest ash or mineral

Table 7
HGI values and coal classification [185].

HGI value	Coal classification
<40	Very hard
40–60	Hard
60–80	Medium hard
80–100	Soft
100–120	Very soft
>120	Extremely soft

content have higher HGI values. This implies that they are softer in grinding. However, contrasting the grindability of the coals based on their ash or mineral composition could not be a fair signal if the rankings of the coals being contrasted are different. Hence, the grindability behaviour is best determined by considering the kind of minerals that the coal contains [184]. The hardgrove grindability index of different biomass based on the different modifications adopted is compared with the HGI of some coals in Table 8. It was generally observed that the HGI value of coal is much more than that of biomass. The HGI values of RB (18–30) were lower compared to the TB (30–55). Some of the HGI values for TB are very close to the HGI values for some coals. The torrefaction of biomass improves its grindability, which makes it easy for its use in pulverized form or for agglomeration with coal as feedstock for power plant operations [41].

8. Microstructure of torrefied biomass

The micrographs of biomass (RB and TB) through scanning electron microscope (SEM) help in the revelation of microstructural changes that could have occurred in the biomass before and after being torrefied [92]. There is a close relationship between the observed phenomenon when FTIR and SEM are used in the characterization of the structural and microstructural changes that occur in the biomass before and post-torrefaction. It has been revealed that the colour of TB transforms into dark brown than RB [190]. A typical example of colour changes as a result of torrefaction condition severity is displayed in Fig. 13.

The increase in carbonization temperature leads to increased dark coloration of the torrefied chips. This increased temperature can cause different structural changes in the biomass. The structural changes ranged from cell structure re-arrangement, surface integration, and tubular-shape structure [142]. Hence, this is an indication of the brittleness of the biomass after torrefaction owing to filaments breakdown in the biomass. Furthermore, the emission of gaseous and volatile products is an indication of the higher total pore volume of the torrefied products over the RB [192]. The gasification and combustion characteristics were improved due to the high porosity of the torrefied product that enables the reactants and products of the carbon matrix [142]. The high porosity in the TB implies low density with constant particle size. Fig. 14(a) gave a deeper examination of the influence of torrefaction on the microstructure of biomass (SCG and CH) [172]. At higher temperature ranges, there were more notable structural changes compared to the RB samples. The most severe torrefaction condition brought about surface degradation of biomass leading to a much scrappier structure owing to more openings and voids on the surface. The cell wall is distorted as well as micro-aperture creations were observed due to torrefied solid surface disintegration. This structural change phenomenon is linked to carbonization and volatile product release of the biomass due to the torrefaction severity conditions such as pretreatment time, reaction temperature, and heating rate. The conditions cause the TB samples to be porous and disintegrated [154]. Fig. 14(b) reveals some of the SEM images of raw coals. The images of the coal raw samples showed that the surfaces were relatively smooth and compact. There was adherence of large amounts of mineral grains on the surface. Coal permeability is reduced as a result of mineral occlusions which have the tendency to block the fluid-flow pathways [148].

Table 8
Biomass type and HGI values.

S/N	Biomass/coal type	HGI	Ref.
1.	Eucalyptus pellets	22	[186]
	Mixed wood pellets	18	
	Miscanthus pellets	18	
	Sunflower pellets	20	
	Steam exploded pellets	29	
2.	Wood pellets	17	[187]
	Straw pellets	20	
	Sunflower husk pellets	22	
	Herbaceous pellets	30	
3.	Torrefied almond shells	30–55	[3]
	Torrefied Kiwifruit pruning	30–55	
	Torrefied pine wood chips	30–55	
4.	Indonesia coal	44	[188]
	Lakhra coal	66	
5.	Punjab coal	57–92	[189]
6.	Black coal	53–87	[185]
7.	Coal 1	94	[184]
	Coal 2	59	
	Coal 3	72	
	Coal 4	64	
8.	21 coal samples	40–130	[77]

9. Torrefied biomass and coal applications in energy

The essence of producing high-energy efficient biomass through torrefaction technique is to be useful in energy-based systems. A pulverized coal boiler was confirmed to be functional when it was fired using 100 % TB without noticeable boiler efficiency declination, boiler load instability, as well as substantial boiler capacity changes [193]. Li et al. [194] and Gil et al. [195] corroborated that the utilization of TB for industrial usage could result in a meaningful reduction of CO_2 and NO_x emissions. Black Wood Technology did the co-firing rate of TB and coal at 5–25 % [196]. It was revealed that TB could replace coal in firing the large-scale plant. Hence, TB introduction in every stage in any system that requires coal, or its derivatives is valuable and advantageous [196]. Few studies have demonstrated the co-combustion of torrefied biomass with coal in existing coal-fired plants using completely new or modified burners as well as mill systems. Smajevic et al. [197] performed trial runs at the Kankaj power station unit 5 with a power output of 110 MW_{el} using two mixtures of brown coal and sawdust. The results confirmed that 7 % sawdust could be combined with brown coal without risking loss in efficiency of the boiler with the additional benefit of reduction of emissions. It was also reported that there was no need for modification of the existing coal transport system and boiler equipment. In another study by Zuwala and Sciazko [198], the co-firing of sawdust, bio-waste, and hard coal was carried out at the Skadina power plant in Poland (1500 MW_{th}). It was reported that 9.5 % biomass was useful to hard coal for efficient co-combustion. The characteristic of torrefied biomass is highly like lean grade coal such that they function effectively in existing coal burners in pilot plants or industrial scale. Molcan et al. [199], Ohliger et al. [200], and Ndibe et al. [201] established that torrefied biomass and coal can be used in co-combustion even at industrial scale plants with even more than 100 kW. Alobaid et al. [202] is one of the recent demonstrations on the use of torrefied biomass and coal for co-combustion in a 1 MW_{th} pulverized coal furnace. The mixture of torrefied biomass and hard coal was co-grinded using the same coal mill though torrefied biomass sharply reduced the throughput of the mill. Yet, there was no difficulty during the co-combustion. The response of mono combustion has no significant variation when compared with co-combustion. Eseyin et al. [203] reported that TB have found applications: as fuel in the combustion chamber of cement kilns and coal-fired power stations. It serves as fuel in burners requiring small-scale pellets as well as in entrained flow gasifiers that require pulverized coal to function. TB is also useful in producing bio-based fuels and chemicals. It is useful as a reducing agent in blast furnace operation. TB can be used in the production of smokeless solid fuels (briquettes, pellets, and more densified products) for various applications domestically and industrially [104]. These are areas where coals have been previously dominant [204], but TB is now fit to replace them partially or totally. Although, in advanced energy applications, no torrefied biomass is comparable to high-graded coal, TB continues to be a verifiable feedstock that is capable of replacing coal in energy-generating systems because they are renewable and environmentally friendly.

Fig. 13. Colour transformation during Patula pine wood chips' torrefaction [191]. Reprinted with approval from Elsevier (License no.: 5502990269268).

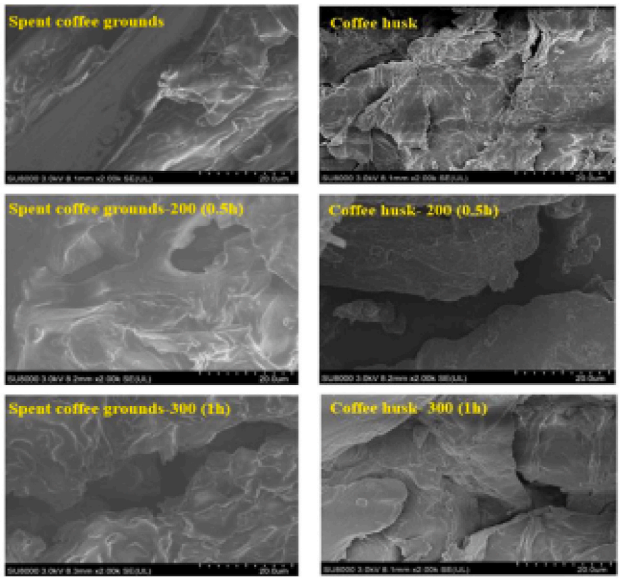

(a)

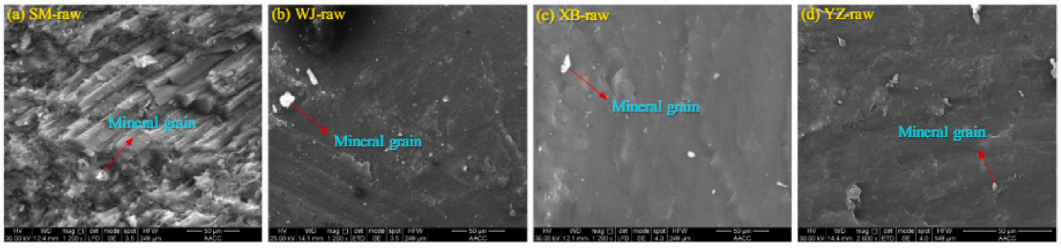

(b)

Fig. 14. SEM of (a) some TB at various torrefaction conditions [172]. (Open access, which permits unrestricted use). (b) Raw coals [148].

10. Conclusions and recommendations

This study has conducted a thorough review of studies relating to torrefied biomass and coals. The characteristics of the two fuels were examined and presented in the review and were juxtaposed. The results were further compared with standards recommended for good and combustible fuels. The study established that because torrefied biomass is renewable and environmentally friendly, it has the potential to replace coal as a viable renewable energy feedstock in energy-generating systems. As a result, it satisfies SDG 7's (clean energy) requirement for eco-friendly environmental materials, making it appropriate for scientists and engineers. The proximate, ultimate, and heating values of torrefied

biomass aligned with those of lean-grade coals that are useful for energy and metallurgical applications. The critical review investigations showed that to a certain extent, torrefied biomass could be a viable substitute for coal in various applications. Hence, the use of torrefied biomass in a mono condition or partially combined with coal for co-combustion purposes is recommended for industrial and domestic uses. Torrefied biomass is economically viable with the combination of scaling up and improving the production technology which helps to improve the product properties. Thus, it is recommended that policy-makers should make biomass prominent as feedstock in co-combustion in co-fired plants for energy generation It will proffer a means to augment the present energy mix, sustainable development, and a pollution-free society.

Author contribution

All authors (Adekunle A. Adeleke, Peter P. Ikubanni, Stephen S. Emmanuel, Moses O. Fajobi, Praise Nwachukwu, Ademidun A. Adesibikan, Jamiu K. Odusote, Emmanuel O. Adeyemi, Oluwaseyi M. Abioye, and Jude A. Okolie) contributed to the scientific writing of the manuscript, while Adeleke A. Adekunle, Jude A. okolie, and Peter P. Ikubanni did the reviewing and editing work.

Declaration of competing interest

The authors declare that they have no known competing financial interests or personal relationships that could have appeared to influence the work reported in this paper.

Data availability

Data will be made available on request.

References

[1] Nimmanterdwong P, Chalermsinsuwan B, Piumsomboon P. Prediction of lignocellulosic biomass structural components from ultimate/proximate analysis. Energy 2021;222:119945. https://doi.org/10.1016/j.energy.2021.119945.

[2] Kabir AR, Anwar SS, Yusup S, Sham DS, Inayat M, Aminu UH. Exploring the potential of coconut shell biomass for charcoal production. Ain Shams Eng J 2022;13:101499. https://doi.org/10.1016/j.asej.2021.05.013.

[3] Nunes LJR. Torrefied biomass as an alternative in coal-fueled power plants: a case study on grindability of agroforestry waste forms. Clean Technol 2020;2(7): 270–89. https://doi.org/10.3390/cleantechnol2030018.

[4] Cabuk B, Duman G, Yanik J, Olgun H. Effect of fuel blend composition on hydrogen yield in co-gasification of coal and non-woody biomass. Int J Hydrog Energy 2020;45:3435–43. https://doi.org/10.1016/j.ijhydene.2019.02.130.

[5] Álvarez-Álvarez P, Pizarro C, Barrio-Anta M, Cámara-Obregón A, Bueno JL, Álvarez A, Gutierrez I, Burslem DFRP. Evaluation of tree species for biomass energy production in northwest Spain. Forests 2018;9:160. https://doi.org/10.3390/f9040160.

[6] Balogun AO, Adeleke AA, Ikubanni PP, Adegoke SO, Alayat AM, McDonald AG. Study on combustion characteristics and thermodynamic parameters of thermal degradation of Guinea grass (*Megathyrsus maximus*) in N_2-pyrolytic and oxidative atmospheres. Sustainability 2022;14:112. https://doi.org/10.3390/su14010112.

[7] Fajobi MO, Lasode OA, Adeleke AA, Ikubanni PP, Balogun AO. Investigation of physicochemical characteristics of selected lignocellulose biomass. Sci Rep 2022; 12:2918. https://doi.org/10.1038/s41598-022-07061-2.

[8] Balogun AO, Adeleke AA, Ikubanni PP, Adegoke SO, Alayat AM, McDonald AG. Thermal decomposition and kinetic modeling of a tropical grass (*Digitaria sanguinalis*) under nitrogen and air environments. Case Stud Therm Eng 2021;26: 101138. https://doi.org/10.1016/j.csite.2021.101138.

[9] Adeleke AA, Odusote JK, Ikubanni PP, Lasode OA, Malathi M, Paswan D. Essential basics on biomass torrefaction, densification and utilization. Int J Energy Res 2021;45:1375–95. https://doi.org/10.1002/er.5884.

[10] Chen WH, Chen CJ, Hung CI, Shen CH, Hsu HW. A comparison of gasification phenomena among raw biomass, torrefied biomass and coal in an entrained-flow reactor. Appl Ener 2013;112:421–30. https://doi.org/10.1016/j.apenergy.2013.01.034.

[11] Chen WH, Lin BJ, Lin YY, Chu YS, Ubando AT, Show PL, Pétrissans M. Progress in biomass torrefaction: principles, applications and challenges. Prog Energy Combust Sci 2021;82:100887.

[12] Thengane SK, Kung KS, Gomez-Barea A, Ghoniem AF. Advances in biomass torrefaction: parameters, models, reactors, applications, deployment, and market. Prog Energy Combust Sci 2022;93:101040.

[13] Tumuluru JS, Ghiasi B, Soelberg NR, Sokhansanj S. Biomass torrefaction process, product properties, reactor types, and moving bed reactor design concepts. Front Energy Res 2021;9:728140.

[14] Castells B, Amez I, Medic L, García-Torrent J. Torrefaction influence on combustion kinetics of Malaysian oil palm wastes. Fuel Process Technol 2021; 218:106843. https://doi.org/10.1016/j.fuproc.2021.106843.

[15] Abdulyekeen KA, Umar AA, Patah MFA, Daud WMAW. Torrefaction of biomass: production of enhanced solid biofuel from municipal solid waste and other types of biomass. Renew Sustain Energy Rev 2021;150:111436. https://doi.org/10.1016/j.rser.2021.111436.

[16] Dhote L, Ganduri J, Kumar S. Evaluation of pyrolysis and gasification of distillery sludge and bio-compost mixed with coal. Fuel 2022;319:123750. https://doi.org/10.1016/j.fuel.2022.123750.

[17] Onokwai AO, Ajisegiri ESA, Okokpujie IP, Ibikunle RA, Oki M, Dirisu JO. Characterization of lignocellulose biomass based on proximate, ultimate, structural composition, and thermal analysis. Mater Today Proc 2022;65: 2156–62. https://doi.org/10.1016/j.matpr.2022.05.313.

[18] Adedeji OM, Russack JS, Molnar LA, Bauer SK. Co-hydrothermal liquefaction of sewage sludge and beverage waste for high-quality bio-energy production. Fuel 2022;324:124757. https://doi.org/10.1016/j.fuel.2022.124757.

[19] Bhattacharjee N, Biswas AB. Physicochemical analysis and kinetic study of orange bagasse at higher heating rates. Fuel 2020;271:117642. https://doi.org/10.1016/j.fuel.2020.117642.

[20] Jiang F, Cao D, Zhang Y, Hu S, Huang X, Ding Y, Wu C, Li J, Ding Y, Liu K. Combustion of the banana pseudo-stem hydrochar by the high-pressure CO_2-hydrothermolysis: thermal conversion, kinetic, and emission analyses. Fuel 2023; 331:125798. https://doi.org/10.1016/j.fuel.2022.125798.

[21] Álvarez A, Migoya S, Menéndez R, Gutiérrez G, Pizarro C, Bueno JL. Torrefaction of short rotation coppice willow. Characterization, hydrophobicity assessment and kinetics of the process. Fuel 2021;295:120601. https://doi.org/10.1016/j.fuel.2021.120601.

[22] Özbay İ, Özbay B, Akdemir U. Biodrying for fuel recovery from sewage sludge: an integrated evaluation by ultimate and proximate analyses. Environ Prog Sustain Energy 2022;41:e13723. https://doi.org/10.1002/ep.13723.

[23] Hongthong S, Raikova S, Leese HS, Chuck CJ. Co-processing of common plastics with pistachio hulls via hydrothermal liquefaction. Waste Manag 2020;102: 351–61. https://doi.org/10.1016/j.wasman.2019.11.03.

[24] Erdoğan S. LHV and HHV prediction model using regression analysis with the help of bond energies for biodiesel. Fuel 2021;301:121065. https://doi.org/10.1016/j.fuel.2021.121065.

[25] Variani VI. Calorific value predicting based on moisture and volatile matter contents using fuzzy inference system. J Phys Conf Ser 2021;1825:012006. https://doi.org/10.1088/1742-6596/1825/1/012006.

[26] Kpalo SY, Zainuddin MF, Halim HBA, Ahmad AF, Abbas Z. Physical characterization of briquettes produced from paper pulp and Mesua ferrea mixtures. Biofuels 2022;13:333–40. https://doi.org/10.1080/17597269.2019.1695361.

[27] Yaka H, Insel MA, Yucel O, Sadikoglu H. A comparison of machine learning algorithms for estimation of higher heating values of biomass and fossil fuels from ultimate analysis. Fuel 2022;320:123971. https://doi.org/10.1016/j.fuel.2022.123971.

[28] García Nieto PJ, García–Gonzalo E, Paredes–Sánchez BM, Paredes–Sánchez JP. Forecast of the higher heating value based on proximate analysis by using support vector machines and multilayer perceptron in bioenergy resources. Fuel 2022; 317:122824. https://doi.org/10.1016/j.fuel.2021.122824.

[29] de Paulo EH, dos Santos FD, Folli GS, Santos LP, Nascimento MHC, Moro MK, da Cunha PHP, Castro EVR, Neto AC, Filgueiras PR. Determination of gross calorific value in crude oil by variable selection methods applied to ^{13}C NMR spectroscopy. Fuel 2022;311:122527. https://doi.org/10.1016/j.fuel.2021.122527.

[30] Bot BV, Sosso OT, Tamba JG, Lekane E, Bikai J, Ndame MK. Preparation and characterization of biomass briquettes made from banana peels, sugarcane bagasse, coconut shells and rattan waste. Biomass Convers Biorefin 2023;13: 7937–46. https://doi.org/10.1007/s13399-021-01762-w.

[31] Inayat M, Sulaiman SA, Naz MY. Thermochemical characterization of oil palm fronds, coconut shells, and wood as a fuel for heat and power generation. MATEC web Conf 2018;225:01008. https://doi.org/10.1051/matecconf/201822501008.

[32] Ibikunle RA, Lukman AF, Titiladunayo IF, Haadi A-R. Modeling energy content of municipal solid waste based on proximate analysis: R-k class estimator approach. Cogent Eng 2022;9:2046243. https://doi.org/10.1080/23311916.2022.2046243.

[33] Saletnik B, Bajcar M, Saletnik A, Zagula G, Puchalski C. Effect of the pyrolysis process applied to waste branches biomass from fruit trees on the calorific value of the biochar and dust explosivity. Energies 2021;14:4898.

[34] Qian C, Li Q, Zhang Z, Wang X, Hu J, Cao W. Prediction of higher heating values of biochar from proximate and ultimate analysis. Fuel 2020;265:116925. https://doi.org/10.1016/j.fuel.2019.116925.

[35] Güleç F, Pekaslan D, Williams O, Lester E. Predictability of higher heating value of biomass feedstocks via proximate and ultimate analyses – a comprehensive study of artificial neural network applications. Fuel 2022;320:123944. https://doi.org/10.1016/j.fuel.2022.123944.

[36] Amen R, Hameed J, Albashar G, Kamran HW, Hassan Shah MU, Zaman MKU, et al. Modelling the higher heating value of municipal solid waste for assessment of waste-to-energy potential: a sustainable case study. J Clean Prod 2021;287: 125575. https://doi.org/10.1016/j.jclepro.2020.125575.

[37] Onifade M, Lawal AI, Aladejare AE, Bada S, Idris MA. Prediction of gross calorific value of solid fuels from their proximate analysis using soft computing and regression analysis. Int J Coal Prep Util 2022;42:1170–84. https://doi.org/10.1080/19392699.2019.1695605.

[38] Qian X, Xue J, Yang Y, Lee SW. Thermal properties and combustion-related problems prediction of agricultural crop residues. Energies 2021;14:4619.

[39] Adegoke SO, Adeleke AA, Ikubanni PP, Nnodim CT, Balogun AO, Falode OA, Adetona So. Energy from biomass and plastics recycling: a review. Cogent Eng 2021;8:1994106. https://doi.org/10.1080/23311916.2021.1994106.

[40] Balogun AO, Adeleke AA, Ikubanni PP, Adegoke SO, Alayat AM, McDonald AG. Kinetics modeling, thermodynamics and thermal performance assessments of pyrolytic decomposition of *Moringa oleifera* husk and *Delonix regia* pod. Sci Rep 2021;11:13862. https://doi.org/10.1038/s41598-021-93407-1.

[41] Adeleke A, Ikubanni P, Odusote J, Orhadahwe T, Lasode O, Adegoke S, Adesina O. Evaluation of non-isothermal kinetic parameters for pyrolysis of teak wood using model-fitting techniques. Trends Sci 2021;18:1432. https://doi.org/10.48048/tis.2021.1432.

[42] Adeleke AA, Ikubanni PP, Odusote JK, Okolie JA, Christopher CT, Orhadahwe TA, Lasode O, Ammasi A. Optimization of densification parameters for lean grade subbituminous Coal. Pet Coal 2022;64:697–708.

[43] Maksimuk Y, Antonava Z, Krouk V, Korsakova A, Kursevich V. Prediction of higher heating value (HHV) based on the structural composition for biomass. Fuel 2021;299:120860. https://doi.org/10.1016/j.fuel.2021.120860.

[44] Ali SA, Sohail TS, Hussain ST, Sadetmahaleh KK, Helmer PT, Haaning NA, Rosendahl LA. Bio-crude production through co-hydrothermal processing of swine manure with sewage sludge to enhance pumpability. Fuel 2021;288:119407. https://doi.org/10.1016/j.fuel.2020.119407.

[45] Ozyuguran A, Akturk A, Yaman S. Optimal use of condensed parameters of ultimate analysis to predict the calorific value of biomass. Fuel 2018;214:640–6. https://doi.org/10.1016/j.fuel.2017.10.082.

[46] Hu X-B, Xu H, Mo W-L, Fan X, Guo W-C, Guo J, Niu J-M, Mi H-Y, Ma Y-Y, Wei X-Y. Effect of sequential thermal dissolution on the structure and pyrolysis characteristics of Naomaohu lignite. Fuel 2023;331:125930. https://doi.org/10.1016/j.fuel.2022.125930.

[47] Mamvura TA, Danha G. Biomass torrefaction as an emerging technology to aid in energy production. Heliyon 2020;6:e03531. https://doi.org/10.1016/j.heliyon.2020.e03531.

[48] Adeleke AA, Odusote JK, Lasode OA, Ikubanni PP, Madhurai M, Paswan D. Evaluation of thermal decomposition characteristics and kinetic parameters of melina wood. Biofuels 2021;13:117–23. https://doi.org/10.1080/17597269.2019.1646541.

[49] Adeleke AA, Ikubanni PP, Balogun AO, Okolie JA, Christopher CT, Olawale AO, Okonkwo JC. Comparative analyses of lean grade coal and carbonized *Antiaris toxicaria* for energy generation. Pet Coal 2022;64:339–49.

[50] Chen D, Gao A, Cen K, Zhang J, Cao X, Ma Z. Investigation of biomass torrefaction based on three major components: hemicellulose, cellulose, and lignin. Energy Convers Manag 2018;169:228–37. https://doi.org/10.1016/j.enconman.2018.05.063.

[51] Mathanker A, Pudasainee D, Kumar A, Gupta R. Hydrothermal liquefaction of lignocellulosic biomass feedstock to produce biofuels: parametric study and products characterization. Fuel 2020;271:117534. https://doi.org/10.1016/j.fuel.2020.117534.

[52] Martínez-Cartas ML, Sánchez S, Cuevas M. Thermal characterization and pyrolysis kinetics of six types of tropical timber from Central Africa. Fuel 2022;307:121824. https://doi.org/10.1016/j.fuel.2021.121824.

[53] Wahab A, Sattar H, Ashraf A, Hussain SN, Saleem M, Munir S. Thermochemical, kinetic and ash characteristics behaviour of Thar Lignite, agricultural residues and synthetic polymer waste (EVA). Fuel 2020;266:117151. https://doi.org/10.1016/j.fuel.2020.117151.

[54] Okati A, Reza Khani M, Shokri B, Monteiro E, Rouboa A. Parametric studies over a plasma co-gasification process of biomass and coal through a restricted model in Aspen plus. Fuel 2023;331:125952. https://doi.org/10.1016/j.fuel.2022.125952.

[55] Lee B-H, Thieu Trinh V, Moon H-B, Lee J-H, Kim H-T, Lee J-W, et al. Physicochemical properties and pyrolysis behavior of petcoke with artificial neural network modeling. Fuel 2023;331:125735. https://doi.org/10.1016/j.fuel.2022.125735.

[56] Kumar P, Kumar Nandi B. Combustion characteristics of high ash Indian coal, wheat straw, wheat husk and their blends. Mater Sci Energy Technol 2021;4:274–81. https://doi.org/10.1016/j.mset.2021.08.001.

[57] Adeleke AA, Ikubanni PP, Odusote JK, Orhadahwe TA, Lasode OA, Adegoke SO, et al. Non-isothermal kinetic parametric evaluation of Tectona grandis using model-fitting methods. Mater Today Proc 2021;44:2874–8. https://doi.org/10.1016/j.matpr.2020.12.1171.

[58] Xu Y-Y, Sun Z-Q, Fan X, Ma F-Y, Kuznetsov PN, Chen B, et al. Building methodology for evaluating the effects of direct coal liquefaction using coal structure-chemical index. Fuel 2021;305:121568. https://doi.org/10.1016/j.fuel.2021.121568.

[59] Singh H, Adeleke AA, Singh C, Ikubanni PP, Orhadahwe TA, Agboola OO. Agglomeration of pet coke and rice straw as mixed fuel for power generation. Pet Coal 2021;63:356–65.

[60] Sher F, Yaqoob A, Saeed F, Zhang S, Jahan Z, Klemeš JJ. Torrefied biomass fuels as a renewable alternative to coal in co-firing for power generation. Energy 2020;209:118444. https://doi.org/10.1016/j.energy.2020.118444.

[61] Trubetskaya A, Leahy JJ, Yazhenskikh E, Müller M, Layden P, Johnson R, Stahl K, Monaghan RFD. Characterization of woodstove briquettes from torrefied biomass and coal. Energy 2019;171:853–65. https://doi.org/10.1016/j.energy.2019.01.064.

[62] Lin Y-L, Zheng N-YT1, Lin Y-L, Zheng N-Y. Torrefaction of fruit waste seed and shells for biofuel production with reduced CO_2 emission. Energy 2021;225:120226. https://doi.org/10.1016/j.energy.2021.120226.

[63] Lin Y-L, Zheng N-Y, Hsu C-H. Torrefaction of fruit peel waste to produce environmentally friendly biofuel. J Clean Prod 2021;284:124676. https://doi.org/10.1016/j.jclepro.2020.124676.

[64] Lee C-G, Kim M-J, Eom C-D. Kinetic study of torrefied woody biomass via TGA using a single heating rate and the model-fitting method. Bioresources 2022;17:411–8. https://doi.org/10.15376/biores.17.1.411-428.

[65] Devaraja UMA, Senadheera SS, Gunarathne DS. Torrefaction severity and performance of rubberwood and gliricidia. Renew Energy 2022;195:1341–53. https://doi.org/10.1016/j.renene.2022.06.109.

[66] Dyjakon A, Sobol Ł, Noszczyk T, Mitręga J. The impact of torrefaction temperature on the physical-chemical properties of residual exotic fruit (Avocado, Mango, Lychee) Seeds. Energies 2022;15:612. https://doi.org/10.3390/en15020612.

[67] Panahi A, Tarakcioglu M, Schiemann M, Delichatsios M, Levendis YA. On the particle sizing of torrefied biomass for co-firing with pulverized coal. Combust Flame 2018;194:72–84. https://doi.org/10.1016/j.combustflame.2018.04.014.

[68] Gajera B, Tyagi U, Sarma AK, Jha MK. Impact of torrefaction on thermal behavior of wheat straw and groundnut stalk biomass: kinetic and thermodynamic study. Fuel Commun 2022;12:100073. https://doi.org/10.1016/j.jfueco.2022.100073.

[69] Nepal R, Kim HJ, Poudel J, Oh SC. A study on torrefaction of spent coffee ground to improve its fuel properties. Fuel 2022;318:123643. https://doi.org/10.1016/j.fuel.2022.123643.

[70] Barbanera M, Muguerza IF. Effect of the temperature on the spent coffee grounds torrefaction process in a continuous pilot-scale reactor. Fuel 2020;262:116493.

[71] Tumsa TZ, Chae TY, Yang W, Paneru M, Maier J. Experimental study on combustion of torrefied palm kernel shell (PKS) in oxy-fuel environment. Int J Energy Res 2019;43:7508–16. https://doi.org/10.1002/er.4792.

[72] Lampropoulos A, Kaklidis N, Athanasiou C, Montes-Morán MA, Arenillas A, Menéndez JA, Binas VD, Konsolakis M, Marnellos GE. Effect of Olive Kernel thermal treatment (torrefaction vs. slow pyrolysis) on the physicochemical characteristics and the CO_2 or H_2O gasification performance of as-prepared biochars. Int J Hydrog Energy 2021;46:29126–41. https://doi.org/10.1016/j.ijhydene.2020.11.230.

[73] Sarker TR, Azargohar R, Dalai AK, Meda V. Enhancement of fuel and physicochemical properties of canola residues via microwave torrefaction. Energy Rep 2021;7:6338–53. https://doi.org/10.1016/j.egyr.2021.09.068.

[74] da Silva JCG, Alves JLF, Mumbach GD, Andersen SLF, Moreira R de FPM, Jose HJ. Torrefaction of low-value agro-industrial wastes using macro-TGA with GC-TCD/FID analysis: physicochemical characterization, kinetic investigation, and evolution of non-condensable gases. J Anal Appl Pyrolysis 2022;166:105607. https://doi.org/10.1016/j.jaap.2022.105607.

[75] Manatura K. Inert torrefaction of sugarcane bagasse to improve its fuel properties. Case Stud Therm Eng 2020;19:100623. https://doi.org/10.1016/j.csite.2020.100623.

[76] Conag AT, Villahermosa JER, Cabatingan LK, Go AW. Predictive HHV model for raw and torrefied sugarcane residues. Waste Biomass Valorization 2019;10:1929–43. https://doi.org/10.1007/s12649-018-0204-2.

[77] Kongto P, Palamanit A, Chaiprapat S, Tippayawong N. Enhancing the fuel properties of rubberwood biomass by moving bed torrefaction process for further applications. Renew Energy 2021;170:703–13. https://doi.org/10.1016/j.renene.2021.02.012.

[78] Singh S, Chakraborty JP, Mondal MK. Torrefaction of woody biomass (*Acacia nilotica*): investigation of fuel and flow properties to study its suitability as a good quality solid fuel. Renew Energy 2020;153:711–24. https://doi.org/10.1016/j.renene.2020.02.037.

[79] Ramos-Carmona S, Martínez JD, Pérez JF. Torrefaction of patula pine under air conditions: a chemical and structural characterization. Ind Crops Prod 2018;118:302–10. https://doi.org/10.1016/j.indcrop.2018.03.062.

[80] Espina RU, Barroca RB, Abundo MLS. Proximate analysis of the torrefied coconut shells. Int J Renew Energy Res 2022;12:489–94. https://doi.org/10.20508/ijrer.v12i1.12902.g8429.

[81] Rahman R, Widodo S, Azikin B, Tahir D. Chemical composition and physical characteristics of coal and mangrove wood as alternative fuel. J Phys Conf Ser 2019;1341:52008. https://doi.org/10.1088/1742-6596/1341/5/052008.

[82] Dobó Z, Fry A. Investigation of co-milling Utah bituminous coal with prepared woody biomass materials in a Raymond bowl mill. Fuel 2018;222:343–9. https://doi.org/10.1016/j.fuel.2018.02.181.

[83] Xiao R, Wang Y, Zhang Y, Xiong Z, Zhang J, Zhao Y. Effect of kaolinite additive on water-soluble sodium release and particle matter formation during Zhundong coal combustion. Fuel 2023;333:126422. https://doi.org/10.1016/j.fuel.2022.126422.

[84] Yelverton TLB, Brashear AT, Nash DG, Brown JE, Singer CF, Kariher PH, Ryan JV, Burnette P. Characterization of emissions from a pilot-scale combustor operating on coal blended with woody biomass. Fuel 2020;264:116774. https://doi.org/10.1016/j.fuel.2019.116774.

[85] Zhang X, Zhu S, Song W, Wang X, Zhu J, Chen R, et al. Experimental study on conversion characteristics of anthracite and bituminous coal during preheating-gasification. Fuel 2022;324:124712.

[86] Wang C, Hou Y, Feng Q, Wang C, Gao X, Che D. Numerical simulation on co-firing ultra-low volatile carbon-based fuels with bituminous coal under oxy-fuel condition. Fuel 2023;332:126087. https://doi.org/10.1016/j.fuel.2022.126087.

[87] Zhang J, Ding Y, Chen W, Li C, Jiao Y. Pyrolysis kinetics, thermodynamics, and interaction analysis of co-pyrolysis of bituminous coal and electrolytic aluminum solid waste. Fuel 2023;333:126375. https://doi.org/10.1016/j.fuel.2022.126375.
[88] Feng Y, Li Y, Zhang X, Su S, Zhang Z, Gan Z, Dong Y. Comparative study on the characteristics of condensable particulate matter emitted from three kinds of coal. Environ Pollut 2021;270:116267. https://doi.org/10.1016/jenvpol.2020.116267.
[89] Fermoso J, Corbet T, Ferrara F, Pettinau A, Maggio E, Sanna A. Synergistic effects during the co-pyrolysis and co-gasification of high volatile bituminous coal with microalgae. Energy Convers Manag 2018;164:399–409. https://doi.org/10.1016/j.enconman.2018.03.023.
[90] Kan H, Wang Y, Mo W-L, Wei X-Y, Mi H-Y, Ma K-J, Zhu M-X, Guo W-C, Guo J, Niu M-J, Fan X. Effect of solvent swelling with different enhancement methods on the microstructure and pyrolysis performance of Hefeng subbituminous coal. Fuel 2023;332:126066. https://doi.org/10.1016/j.fuel.2022.126066.
[91] Bai B, Qiang L, feng S, Mu H, Ma X. Influence of coal structure change caused by different pretreatment methods on Shengli lignite pyrolysis. Fuel 2023;332:126089. https://doi.org/10.1016/j.fuel.2022.126089.
[92] Wang Y, Zhou Y, Bai N, Han J. Experimental investigation of the characteristics of NOx emissions with multiple deep air-staged combustion of lean coal. Fuel 2020;280:118416. https://doi.org/10.1016/j.fuel.2020.118416.
[93] Wu L, Guan Y, Zhou J, Jiang X, Liu T, Pan J. Effects of variable amounts of volatiles in corncob on microwave co-pyrolysis of low-rank coal and corncob. Fuel 2023;332:126133. https://doi.org/10.1016/j.fuel.2022.126133.
[94] Kanwal S, Chaudhry N, Munir S, Sana H. Effect of torrefaction conditions on the physicochemical characterization of agricultural waste (sugarcane bagasse). Waste Manag 2019;88:280–90. https://doi.org/10.1016/j.wasman.2019.03.053.
[95] Trinh VT, Jeong T-Y, Lee B-H, Jeon C-H. Comparative study of the synergistic effects of blending raw/torrefied biomass and Vietnamese anthracite using Co-pyrolysis. ACS Omega 2021;6:29171–83. https://doi.org/10.1021/acsomega.1c04610.
[96] Kim SJ, Park S, Oh KC, Ju YM, Cho L hoon, Kim DH. Development of surface torrefaction process to utilize agro-byproducts as an energy source. Energy 2021;233:121192. https://doi.org/10.1016/j.energy.2021.121192.
[97] Bajcar M, Zaguła G, Saletnik B, Tarapatskyy M, Puchalski C. Relationship between torrefaction parameters and physicochemical properties of torrefied products obtained from selected plant biomass. Energies 2018;11:2919. https://doi.org/10.3390/en11112919.
[98] Cahyanti MN, Doddapaneni TRKC, Madissoo M, Pärn L, Virro I, Kikas T. Torrefaction of agricultural and wood waste: comparative analysis of selected fuel characteristics. Energies 2021;14:2774. https://doi.org/10.3390/en14102774.
[99] Buratti C, Tumsaera M, Lascaro E, Cotana F. Optimization of torrefaction conditions of coffee industry residues using desirability function approach. Waste Manag 2018;73:523–34. https://doi.org/10.1016/j.wasman.2017.04.012.
[100] Zhang C, Yang W, Chen W-H, Ho S-H, Pétrissans A, Pétrissans M. Effect of torrefaction on the structure and reactivity of rice straw as well as life cycle assessment of torrefaction process. Energy 2022;240:122470. https://doi.org/10.1016/j.energy.2021.122470.
[101] Xin H, Zhou B, Tian W, Qi X, Zheng M, Lu W, Yang H, Zhong X, Wang D. Pyrolytic stage evolution mechanism of Zhundong coal based on reaction consistency analysis of mono/multi molecular models. Fuel 2023;333:126371. https://doi.org/10.1016/j.fuel.2022.126371.
[102] Adeleke AA, Odusote JK, Ikubanni PP, Olabisi AS, Nzerem P. Briquetting of subbituminous coal and torrefied biomass using bentonite as inorganic binder. Sci Rep 2022;12:8716. https://doi.org/10.1038/s41598-022-12685-5.
[103] Adeleke A, Odusote J, Ikubanni P, Lasode O, Malathi M, Pasawan D. Physical and mechanical characteristics of composite briquette from coal and pretreated wood fines. Int J Coal Sci Technol 2021;8:1088–98.
[104] Adeleke AA, Odusote JK, Ikubanni PP, Agboola OO, Balogun AO, Lasode OA. Tumbling strength and reactivity characteristics of hybrid fuel briquette of coal and biomass wastes blends. Alexandria Eng J 2021;60:4619–25. https://doi.org/10.1016/j.aej.2021.03.069.
[105] Adeleke AA, Odusote JK, Lasode OA, Ikubanni PP, Malathi M, Paswan D. Densification of coal fines and mildly torrefied biomass into composite fuel using different organic binders. Heliyon 2019;5:e02160. https://doi.org/10.1016/j.heliyon.2019.e02160.
[106] Sermyagina E, Mendoza C, Deviatkin I. Effect of hydrothermal carbonization and torrefaction on spent coffee grounds. Agronomy Res 2021;19:928–43. https://doi.org/10.15159/AR.21.023.
[107] Pahla G, Mamvura TA, Muzenda E. Torrefaction of waste biomass for application in energy production in South Africa. South African. J Chem Eng 2018;25:1–12. https://doi.org/10.1016/j.sajce.2017.11.003.
[108] Adeleke AA, Odusote JK, Ikubanni PP, Lasode OA, Malathi M, Paswan D. The ignitability, fuel ratio and ash fusion temperatures of torrefied woody biomass. Heliyon 2020;6:e03582. https://doi.org/10.1016/j.heliyon.2020.e03582.
[109] Chen Y-C, Jhou S-Y. Integrating spent coffee grounds and silver skin as biofuels using torrefaction. Renew Energy 2020;148:275–83. https://doi.org/10.1016/j.renene.2019.12.005.
[110] Chen D, Gao A, Ma Z, Fei D, Chang Y, Shen C. In-depth study of rice husk torrefaction: characterization of solid, liquid and gaseous products, oxygen migration and energy yield. Bioresour Technol 2018;253:148–53. https://doi.org/10.1016/j.biortech.2018.01.009.
[111] Tsai W-T, Jiang T-J, Tang M-S, Chang C-H, Kuo T-H. Enhancement of thermochemical properties on rice husk under a wide range of torrefaction conditions. Biomass Convers Biorefinery 2021. https://doi.org/10.1007/s13399-021-01945-5.
[112] Poudel J, Karki S, Oh SC. Valorization of waste wood as a solid fuel by torrefaction. Energies 2018;11:1641. https://doi.org/10.3390/en11071641.
[113] Adeleke AA, Odusote JK, Lasode OA, Ikubanni PP, Malathi M, Paswan D. Mild pyrolytic treatment of Gmelina arborea for optimum energetic yields. Cogent Eng 2019;6:1593073. https://doi.org/10.1080/23311916.2019.15933073.
[114] Ajimotokan HA, Ehindero AO, Ajao KS, Adeleke AA, Ikubanni PP, Shuaib-Babata YL. Combustion characteristics of fuel briquettes made from charcoal particles and sawdust agglomerates. Sci Afr 2019;6:e00202. https://doi.org/10.1016/j.sciaf.2019.e00202.
[115] Ibitoye SE, Jen T-C, Mahamood RM, Akinlabi ET. Improving the combustion properties of corncob biomass via torrefaction for solid fuel applications. J Compos Sci 2021;5:260. https://doi.org/10.3390/jcs5100260.
[116] Aich S, Behera D, Nandi BK, Bhattacharya S. Relationship between proximate analysis parameters and combustion behaviour of high ash Indian coal. Int J Coal Sci Technol 2020;7:766–77. https://doi.org/10.1007/s40789-020-00312-5.
[117] Hadi K, Ichimura R, Hashimoto G, Xia Y, Hashimoto N, Fujita O. Effect of fuel ratio of coal on the turbulent flame speed of ammonia/coal particle cloud co-combustion at atmospheric pressure. Proc Combust Inst 2021;38:4131–9. https://doi.org/10.1016/j.proci.2020.06.358.
[118] Aich S, Nandi BK, Bhattacharya S. Effect of weathering on physico-chemical properties and combustion behavior of an Indian thermal coal. Int J Coal Sci Technol 2019;6:51–62. https://doi.org/10.1007/s40789-018-0235-0.
[119] Lin Y-L, Zheng N-Y, Lin C-S. Repurposing *Washingtonia filifera* petiole and *Sterculia foetida* follicle waste biomass for renewable energy through torrefaction. Energy 2021;223:120101. https://doi.org/10.1016/j.energy.2021.120101.
[120] Rago YP, Collard F-X, Görgens JF, Surroop D, Mohee R. Torrefaction of biomass and plastic from municipal solid waste streams and their blends: evaluation of interactive effects. Fuel 2020;277:118089. https://doi.org/10.1016/j.fuel.2020.118089.
[121] Singh S, Chakraborty JP, Mondal MK. Optimization of process parameters for torrefaction of *Acacia nilotica* using response surface methodology and characteristics of torrefied biomass as upgraded fuel. Energy 2019;186:115865. https://doi.org/10.1016/j.energy.2019.118089.
[122] Singh RK, Sarkar A, Chakraborty JP. Effect of torrefaction on the physicochemical properties of pigeon pea stalk (Cajanus cajan) and estimation of kinetic parameters. Renew Energy 2019;138:805–19. https://doi.org/10.1016/j.renene.2019.02.022.
[123] Wang C, Tang G, Sun R, Hu G, Yuan M, Che D. The correlations of chemical property, alkali metal distribution, and fouling evaluation of Zhundong coal. J Energy Inst 2020;93:2204–14. https://doi.org/10.1016/j.joei.2020.06.002.
[124] Adeleke AA, Odusote JK, Paswan D, Lasode OA, Malathi M. Influence of torrefaction on lignocellulosic woody biomass of Nigerian origin. J Chem Technol Metall 2019;54:274–85.
[125] Zhang J, Jia X, Wang C, Zhao N, Wang P, Che D. Experimental investigation on combustion and NO formation characteristics of semi-coke and bituminous coal blends. Fuel 2019;247:87–96. https://doi.org/10.1016/j.fuel.2019.03.045.
[126] Lee B-H, Sh L, Lee D-G, Jeon C-H. Effect of torrefaction and ashless process on combustion and NO_x emission behaviors of woody and herbaceous biomass. Biomass Bioenergy 2021;151:106133. https://doi.org/10.1016/j.biombioe.2021.106133.
[127] Zając G, Szyszlak-Bargłowicz J, Gołębiowski W, Szczepanik M. Chemical characteristics of biomass ashes. Energies 2018;11:2885. https://doi.org/10.3390/en11112885.
[128] Adeleke AA, Ikubanni PP, Orhadahwe TA, Christopher CT, Akano JM, Agboola OO, Adegoke SO, Balogun AO, Ibikunle RA. Sustainability of multifaceted usage of biomass: a review. Heliyon 2021;7:e08025. https://doi.org/10.1016/j.heliyon.2021.e08025.
[129] Yin C. Development in biomass preparation for suspension firing towards higher biomass shares and better boiler performance and fuel rangeability. Energy 2020;196:117129. https://doi.org/10.1016/j.energy.2020.117129.
[130] Margaritis N, Grammelis P, Karampinis E, Kanaveli I-P. Impact of torrefaction on vine Pruning's fuel characteristics. J Energy Eng 2020;146:4020006. https://doi.org/10.1061/(ASCE)EY.1943-7897.0000654.
[131] Zhang Y, Zhao J, Ma Z, Yang F, Cheng F. Effect of oxygen concentration on oxy-fuel combustion characteristic and interactions of coal gangue and pine sawdust. Waste Manag 2019;87:288–94. https://doi.org/10.1016/j.wasman.2019.01.040.
[132] Doddapaneni TRKC, Pärn L, Kikas T. Torrefaction of pulp industry sludge to enhance its fuel characteristics. Energies 2022;15:6175. https://doi.org/10.3390/en15176175.
[133] Jagodzińska K, Gądek W, Pronobis M, Kalisz S. Investigation of ash deposition in PF boiler during combustion of torrefied biomass. IOP Conf Ser Earth Environ Sci 2019;214:012080. https://doi.org/10.1088/1755-1315'214/1/012080.
[134] Lebendig F, Funcia I, Pérez-Vega R, Müller M. Investigations on the effect of pre-treatment of wheat straw on ash-related issues in chemical looping gasification (CLG) in comparison with woody biomass. Energies 2022;15:3422. https://doi.org/10.3390/en15093422.
[135] Kim G-M, Lisandy KY, Isworo YY, Kim J-H, Jeon C-H. Investigation into the effects of ash-free coal binder and torrefied biomass addition on coke strength and reactivity. Fuel 2018;212:487–97. https://doi.org/10.1016/j.fuel.2017.10.077.
[136] Zhang W, Sun S, Zhu H, Zhang L, Zhao Y, Wang P. The evolution characteristics of bituminous coal in the process of pyrolysis at elevated pressure. Fuel 2021;302:120832. https://doi.org/10.1016/j.fuel.2021.120832.

[137] Adeleke AA, Odusote JK, Ikubanni PP, Orhadahwe TA, Lasode OA, Ammasi A, Kumar K. Ash analyses of bio-coal briquettes produced using blended binder. Sci Rep 2021;11:547. https://doi.org/10.1038/s41598-020-79510-9.
[138] Lu G, Zhang K, Cheng F. The fusion characteristics of ashes from anthracite and biomass blends. J Energy Inst 2018;91:797–804. https://doi.org/10.1016/j.joei.2017.05.001.
[139] Oladejo JM, Adegbite S, Pang C, Liu H, Lester E, Wu T. In-situ monitoring of the transformation of ash upon heating and the prediction of ash fusion behaviour of coal/biomass blends. Energy 2020;199:117330. https://doi.org/10.1016/j.energy.2020.117330.
[140] Li F, Yu B, Wang G, Fan H, Wang T, Guo M, et al. Investigation on improve ash fusion temperature (AFT) of low-AFT coal by biomass addition. Fuel Process Technol 2019;191:11–9. https://doi.org/10.1016/j.fuproc.2019.03.005.
[141] Ni Y, Hu S, Zhang Y, Zhang M, Li H, Zhou H. Research on the effects of the fly ash reburning on element migration and ash deposition characteristics of high-alkali coal in a full-scale slag-tapping boiler. Fuel 2023;335:126952. https://doi.org/10.1016/j.fuel.2022.126952.
[142] Niu Y, Lv Y, Zhang X, Wang D, Li P. Effects of water leaching (simulated rainfall) and additives (KOH, KCl, and SiO_2) on the ash fusion characteristics of corn straw. Appl Therm Eng 2019;154:485–92.
[143] Liu Z, Zhang T, Zhang J, Xiang H, Yang X, Hu W, Liang F, Mi B. Ash fusion characteristics of bamboo, wood and coal. Energy 2018;161:517–22. https://doi.org/10.1016/j.energy.2018.07.131.
[144] Ünlü N, Özdoğan S. Entrained flow Co-gasification of torrefied biomass and coal. Energy 2023;263:125864. https://doi.org/10.1016/j.energy.2022.125864.
[145] Rodrigues A, Nunes LJR. Evaluation of ash composition and deposition tendencies of biomasses and torrefied products from woody and shrubby feedstocks: SRC poplar clones and common broom. Fuel 2020;269:117454. https://doi.org/10.1016/j.fuel.2020.117454.
[146] Emmanuel SS, Adesibikan AA, Saliu OD. Phytogenically bioengineered metal nanoarchitecture for degradation of refractory dye water pollutants: a pragmatic minireview. Appl Organomet Chem 2023;37:e6946. https://doi.org/10.1002/aoc.6946.
[147] Jiang J, Zhang S, Longhurst P, Yang W, Zheng S. Molecular structure characterization of bituminous coal in Northern China via XRD, Raman and FTIR spectroscopy. Spectrochim Acta Part A Mol Biomol Spectrosc 2021;255:119724. https://doi.org/10.1016/j.saa.2021.119724.
[148] Li H, Shi S, Lin B, Lu J, Ye Q, Lu Y, Wang Z, Hong Y, Zhu X. Effects of microwave-assisted pyrolysis on the microstructure of bituminous coals. Energy 2019;187:115986. https://doi.org/10.1016/j.energy.2019.115986.
[149] Patidar K, Vashishtha M. Impact of torrefaction conditions on the physicochemical properties of mustard crop residue. Mater Today Proc 2021;44:4072–8. https://doi.org/10.1016/j.matpr.2020.10.445.
[150] Jaideep R, Lo WH, Lim GP, Chua CX, Gan S, Lee LY, Thangalazhy-Gopakumar S. Enhancement of fuel properties of yard waste through dry torrefaction. Mater Sci Energy Technol 2021;4:156–65. https://doi.org/10.1016/j.mset.2021.04.001.
[151] Jiang J, Yang W, Cheng Y, Liu Z, Zhang Q, Zhao K. Molecular structure characterization of middle-high rank coal via XRD, Raman and FTIR spectroscopy: implications for coalification. Fuel 2019;239:559–72. https://doi.org/10.1016/j.fuel.2018.11.057.
[152] Yan J, Lei Z, Li Z, Wang Z, Ren S, Kang S, et al. Molecular structure characterization of low-medium rank coals via XRD, solid state 13C NMR and FTIR spectroscopy. Fuel 2020;268:117038. https://doi.org/10.1016/j.fuel.2020.117038.
[153] Cheng X, Huang Z, Wang Z, Ma C, Chen S. A novel on-site wheat straw pretreatment method: enclosed torrefaction. Bioresour Technol 2019;281:48–55. https://doi.org/10.1016/j.biortech.2019.02.075.
[154] Sarker TR, Azargohar R, Dalai AK, Venkatesh M. Physicochemical and fuel characteristics of torrefied agricultural residues for sustainable fuel production. Energy Fuels 2020;34:14169–81. https://doi.org/10.1021/acs.energyfuels.0c02121.
[155] Giang DK, Ban SE, Choi JH, Seong H, Jung CD, Kim H, Lee JW. Effect of torrefied biomass on hydrophobicity and mechanical properties of polylactic acid composites. Int J Biol Macromol 2022;215:36–44.
[156] Odusote JK, Adeleke AA, Lasode OA, Malathi M, Paswan D. Thermal and compositional properties of treated Tectona grandis. Biomass Convers Biorefinery 2019;9:511–9. https://doi.org/10.1007/s13399-019-00398-1.
[157] Wang S, Dai G, Ru B, Zhao Y, Wang X, Xiao G, Luo Z. Influence of torrefaction on the characteristics and pyrolysis behaviour of cellulose. Energy 2017;120:864–71. https://doi.org/10.1016/j.energy.2016.11.135.
[158] Law KY. Definition of hydrophilicity, hydrophobicity and superhydrophobicity: getting the basics right. J Phys Chem Lett 2014;5(4):686–8. https://doi.org/10.1021/jz402762h.
[159] Chen D, Gao A, Cen K, Zhang J, Cao X, Ma Z. Investigation of biomass torrefaction based on three major components: hemicellulose, cellulose, and lignin. Energy Convers Manag 2018;169:228–37. https://doi.org/10.1016/j.enconman.2018.05.063.
[160] Chen WH, Peng J, Bi XT. A state-of-the-art review of biomass torrefaction, densification and applications. Renew Sust Energy Reviews 2015;44:847–66. https://doi.org/10.1016/j.rser.2014.12.039.
[161] Tumuluru JS, Ghiasi B, Soelberg NR, Sokhansanj S. Biomass torrefaction process, product propertie, reactor types, and moving bed reactor design concepts. Front Energy Res 2021;9:728140. https://doi.org/10.3389/fenrg.2021.728140.
[162] Messay EG, Birhanu AA, Mulissa JM, Genet TA, Endale WA, Gutema BF. Briquette production from sugar cane bagasse and its potential as clean source of energy. African J Environ Sci Technol 2021;15:339–48. https://doi.org/10.5897/ajest2021.3006.
[163] Zhang Y, Chen F, Chen D, Cen K, Zhang J, Cao X. Upgrading of biomass pellets by torrefaction and its influence on the hydrophobicity, mechanical property and fuel quality. Biomass Convers Biorefin 2022;12:2061–70. https://doi.org/10.1007/s13399-020-00666-5.
[164] Acharjee TC, Coronella CJ, Vasquez VR. Effect of thermal pretreatment on equilibrium moisture content of lignocellulosic biomass. Biores Technol 2011;102:4849–54.
[165] Wen JL, Sun SL, Yuan TQ, Xu F, Sun RC. Understanding the chemical and structural transformations of lignin macromolecule during torrefaction. Appl Energy 2014;121:1–9. https://doi.org/10.1016/j.apenergy.2014.02.001.
[166] Dyjakon A, Noszczyk T, Smedzik M. The influence of torrefaction temperature in hydrophobic properties of waste biomass from food processing. Energies 2019;12:4609. https://doi.org/10.3390/en12244609.
[167] Ahmad MI, Rizman ZI, Rasat MSM, Alauddin ZAZ, Soid SNM, Aziz MSA, Mohamed M, Amini MHM, Amin MFM. The effect of torrefaction on oil palm empty fruit bunch properties using microwave irradiation. J Fundamental Appl Sci 2017;9:924–40. https://doi.org/10.4314/jfas.v9i3s.67.
[168] Matali S, Rahman NA, Idris SS, Yaacob N, Alias AB. Lignocellulosic biomass solid fuel properties enhancement via torrefaction. Procedia Eng 2016;148:671–8. https://doi.org/10.1016/j.proeng.2016.06.550.
[169] Keeratiisariyakul P, Rousset P, Pattiya A. Coupled effect of torrefaction and densification pre-treatment on biomass energetic and physical properties. J Sustain Energy Environ 2019;10:1–10.
[170] Dyjakon A, Noszczyk T. Alternative fuels from forestry biomass residue: torrefaction process of Horse chestnuts, Oak acorns and spruce cones. Energies 2020;13:2468. https://doi.org/10.3390/en13102468.
[171] Prasongthum N, Duangwongsa N, Khowattana P, Suemanotham A, Wongharn P, Thanmongkhon Y, Reubroycharoen P, Attanatho L. Influence of torrefaction on yields and characteristics of densified solid biofuel. J Phys Conf Series 2022;2175:1–9. https://doi.org/10.1088/1742-6596/2175/1/012027.
[172] Mukherjee A, Okolie JA, Niu C, Dalai AK. Experimental and modeling studies of torrefaction of spent coffee ground and coffee husk: effects on surface chemistry and carbon dioxide capture performance. ACS Omega 2022;7(1):638–53. https://doi.org/10.1021/acsomega.1c05270.
[173] Surono UB, Saptoadi H, Rohmat TA. Improving thermochemical and physical properties of coca pod shell by torrefaction and its potential utilization. Int Energy J 2020;20:141–54.
[174] Aamiri OB, Thilakaratne R, Tumuluru JS, Satyavolu J. An “in-situ bonding” approach to produce torrefied biomass briquetes. Bioengineering 2019;6:87. https://doi.org/10.3390/bioengineering6040087.
[175] Riaz S, Al-Abdeli Y. Effects of constant and staged torrefaction temperatures on biomass combustion and pyrolysis. Nov. 21 -24. In: Proceeding of the Australian combustion symposium 2021; 2021. Toowoomba, Queensland, pp. 181 – 185, https://anz-combustioninstitute.org/ACS2021/proceedings.php.
[176] Jeong JS, Kim GM, Jeong HJ, Kim GB, Jeon CH. A study on the improved the hydrophobicity of torrefied biomass. Trans Korean Hydrog New Energy Society 2019;30:49–57. https://doi.org/10.7316/KHNES.2019.30.1.49.
[177] Junga R, Pospolita J, Niemiec P. Combustion and grindability characteristics of palm kernel shells torrefied in a pilot-scale installation. Renew Energy 2020;147:1239–50. https://doi.org/10.1016/j.renene.2019.09.060.
[178] Manuochehrinejad M, van Giesen I, Mani S. Grindability of torrefied wood chips and wood pellets. Fuel Process Technol 2018;182:45–55. https://doi.org/10.1016/j.fuproc.2018.10.015.
[179] Temmerman M, Jesen J, Herbert J. Von Rittinger theory adapted to wood chip and pellet milling in a laboratory scale hammermill. Biomass Bioenergy 2013;56:70–81. https://doi.org/10.1016/j.biombioe.2013.04.020.
[180] Dyjakon A, Noszczyk T, Mostek A. Mechanical durability and grindability of pellets after torrefaction process. Energies 2021;14. https://doi.org/10.3390/en14206772. 6772.
[181] Telte W, Nielsen NPK, Hansen HO, Dahl J, Shang L, Sanadi AR. Pelletizing properties of torrefied wheat straw. Biomass Bioenergy 2013;49. https://doi.org/10.1016/j.biombioe.2012.12.025. 214–221.
[182] Yu S, Park J, Kim M, Kim H, Ryu C, Lee Y, Yang W, Jeong Y. Improving energy density and grindability of wood pellets by dry torrefaction. Energy Fuels 2019;33:8632–9.
[183] Phanphanich M, Mani S. Impact of torrefaction on the grindability and fuel characteristics of forest biomass. Biores Technol 2011;102:1246–52. https://doi.org/10.1016/j.biortech.2010.08.028.
[184] Idris A, Man Z, Bustam A, Rabat NE, Uddin F, Abdul Mannan H. Grindability and abrasive behavior of coal blends: analysis and prediction. Int J Coal Preparation Utilizat 2019;42:1143–69.
[185] Tichánek F. Contribution to determination of coal grindability using hardgrove method. GeoScience Engineering 2008;54:27–32.
[186] Williams O, Taylor S, Lester E, Kingman S, Giddings D, Eastwick C. Applicability of mechanical tests for biomass pellet characterisation for bioenergy applications. Materials 2018;1:1–18. https://doi.org/10.3390/ma11081329.
[187] Tymoszuk M, Mroczek K, Kalisz S, Kubiczek H. An investigation of biomass grindability. Energy 2019;183:116–26. https://doi.org/10.1016/j.energy.2019.05.167.
[188] Shahani NM. An assessment of the effect of coal blending on hardgrove grindability index. Petroleum and Coal 2019;61:269–76.
[189] Shahzad M, Iqbal MM, Hassan SA, Saqib S, Waqas M. An assessment of chemical properties and hardgrove grindability index of Punjab coal. Pakistan J Sci Indus Res Series A Phys Sci 2014;57:139.

[190] Pimchuai A, Dutta A, Basu P. Torrefaction of agriculture residue to enhance combustible properties. Energy Fuel 2010;24:4638–45. https://doi.org/10.1021/ef901168f.
[191] Ramos-Carmona S, Delgado-Balcázar S, Perez JF. Physicochemical characterization of torrefied wood biomass under air as oxidizing atmosphere. Bioresources 2017;12(3):5428–48.
[192] Chen Q, Zhou JS, Liu BJ, Mei QF, Luo ZY. Influence of torrefaction pretreatment on biomass gasification technology. Chin Sci Bull 2011;56:1449–56. https://doi.org/10.1007/s11434-010-4292-z.
[193] Rousset P, Fernandes K, Vale A, Macedo L, Benoist A. Change in particle size distribution of Torrefied biomass during cold fluidization. Energy 2013;51(1):71–7. https://doi.org/10.1016/j.energy.2013.01.030.
[194] Li J, Brzdekiewicz A, Yang W, Blasiak W. Co-firing based on biomass torrefaction in a pulverized coal boiler with aim of 100% fuel switching. Appl Energy 2012;99:344–54. https://doi.org/10.1016/j.apenergy.2012.05.046.
[195] Gil MV, García R, Pevida C, Rubiera F. Grindability and combustion behavior of coal and torrefied biomass blends. Biores Technol 2015;191:205–12. https://doi.org/10.1016/j.biortech.2015.04.117.
[196] Proskurina S, Heinimö J, Schipfer F, Vakkilainen E. Biomass for industrial applications: the role of torrefaction. Renew Energy 2017;111:265–74. https://doi.org/10.1016/j.renene.2017.04.015.
[197] Smajevic I, Kazagi A, Music M, Becic K, Hasanbegovic I, Sokolovic S, Delihasanovic N, Skopljak A, Hodzic N. Co-firing Bosnian coals with woody biomass: experimental studies on a laboratory sacle furnace and 110 MWe power unit. Thermal Sci 2012;16:789–804. https://doi.org/10.2298/TSCI120120122S.
[198] Zuwala J, Sciazko M. Full-scale co-firing trial tests of sawdust and bio-waste in pulverized coal-fired steam boiler. Biomass Bioenergy 2010;34(8):1165–74. https://doi.org/10.1016/j.biombioe.2010.03.003.
[199] Molcan P, Lu G, Le Bris T, Yan Y, Taupin B, Caillat S. Characterisation of biomass and coal co-firing on a 3 MW_{th} combustion test facility using fame imagining and Gas/ash sampling techniques. Fuel 2009;88:2328–34. https://doi.org/10.1016/j.fuel.2009.06.027.
[200] Ohliger A, Christ D, Heil P, Forster M, Kneer R. Biomasse -torrefizierung und anschlebende mitverbrennung in Luft-und Oxyfuelatmosphere, 25 Duetscher flamentag. Karlsruhe: VDI Verlag; 2011. p. 365–70.
[201] Ndibe C, Grathwohl S, Paneru M, Maier J, Scheffknecht G. Emissions reduction and deposits characteristics during cofiring of high shares of tirrefied biomass in a 500 kW pulverized coal furnace. Fuel 2015;156:177–89. https://doi.org/10.1016/j.fuel.2015.04.017.
[202] Alobaid F, Busch JP, Syroh A, Strohle J, Epple B. Experimental measurements for torrefied biomass co-combustion in a 1 MW_{th} pulverized coal-fired furnace. J Energy Inst 2020;93:833–46. https://doi.org/10.1016/j.joei.2019.07.008.
[203] Eseyin AE, Steele PH, Pittman Jr. CU. Current trends in the production and applications of torrefied wood/biomass - a review. Bioresources 2015;10:8812–58. https://doi.org/10.15376/biores.10.4.8812-8858.
[204] Ikubanni PP, Adeleke AA, Agboola OO, Adesina OS, Nnodim CT, Balogun AO, Okonkwo CJ, Olawale AO. Characterization of some commercially available Nigerian coals as carbonaceous material for direct reduced iron production. Mater Today Proc 2021;44:2849–54. https://doi.org/10.1016/j.matpr.2020.12.1167.